E-gel Films and Natural Silk Mats: Novel Processes for the Creation of Functional Silk Surfaces

A thesis

submitted by

Jason Edward Bressner

In partial fulfillment of the requirements
for the degree of

Master of Science

in

Biomedical Engineering

T U F T S U N I V E R S I T Y

August 2011

Adviser:

Prof. Fiorenzo G. Omenetto

ABSTRACT

Silk is a material with a history dating back thousands of years. Despite this precedent, the past few years have witnessed the launch of a new silk renaissance, one that leverages our ability to solubilize and reform silk cocoons to create materials including films, gels, and tissue engineering scaffolds. Further, these products are easily functionalized through the direct addition of chemical or biological agents in solution. Two techniques that are introduced here represent new approaches for the fabrication of functional silk surfaces: E-gel films and natural silk mats.

E-gel films rely upon the application of direct current to a regenerated silk solution while using a ring-shaped anode. Notably, this approach allows for films with a range of three-dimensional topologies to be formed, with exceptionally low surface roughness on the order of Angstroms.

Natural silk mats are spun directly by the silkworm through influencing its innate behavior, constraining the heights available for the creation of anchor points. A threshold height is approximated below which silkworms will spin flat sheets and above which they will encapsulate themselves in cocoons. Furthermore, the resulting mats can be functionalized through the addition of drugs, dyes, and other molecules directly to the silkworm's mulberry leaf-based diet. Functional materials, including antibacterial silk, were produced and validated in this study.

ACKNOWLEDGEMENTS

This work contained in this thesis never would have been completed without the support of a legion of people to whom I owe a debt of thanks.

First and foremost, I would like to thank my family for the role that they have played throughout this journey. My parents, Robert and Carmen Bressner, my late grandparents, Joseph and Nettie Bressner, my aunt, Dona Schwab and my uncle, Jerry Bressner, all fostered my pursuit of knowledge and love for science from a young age. Moreover, they instilled in me a sense of compassion that has guided me in my pursuits and given purpose to work whose goal is to help others.

Throughout this span as a graduate student, my wife, Yasmeen Bressner, also has been a tremendous source of love and encouragement. More recently, she has blessed our family with two children, Jonah and Amira, who inspire me every day.

At Tufts, I have enjoyed the privilege of working with some extremely talented people, and I have learned a great deal from their examples. Post-docs Jamey Moeser, Pete Domachuk, Jessica Mondia and Hu 'Tiger' Tao from the Omenetto Lab as well as Graham Tilburey, Nik Kojic, Guokui Qin and Eleanor Pritchard from the Kaplan Lab have helped me in my efforts and enabled me to understand

how I might become a better researcher. Additionally, Yuji Zhang, Taylor Williams, Nick Guziewicz, Brian Lawrence, Kosta Tsioris, Debbie Chen, Mike Curtis, Alex Nectow and Alex Mitropoulos have been fellow graduate students with whom I have enjoyed countless discussions, both scientific and otherwise. I thank them all for their assistance and their friendship. Finally, I am grateful to Lauren Klinker, currently a rising senior at the College, who spent over a year working with me, with extraordinary energy and enthusiasm, on silk optical fibers and subsequently on e-gel films.

In addition, there are a few faculty members who must be recognized for their contributions. Mark Cronin-Golomb has been a valuable resource, readily available to act as a sounding board for a number of my ideas and to pose thought-provoking questions. Matt Panzer, from the Chemical and Biological Engineering department, shared his expertise in electrochemistry and opened his lab to me in trying to make e-gel films whose thicknesses approached a single wavelength of visible light.

Finally, I would like to thank my committee: adviser Fiorenzo Omenetto, BME department chair David Kaplan, and Mechanical Engineering professor Gary Leisk. From the first course of his that I took, David encouraged me to think about research in very practical terms and to appreciate how vision, to be

meaningful, must be well-articulated and compelling in the context of related work as well as the broader scientific community. Gary introduced me to electrogelation, initially as one vital step in a more elaborate method to produce silk fibers. This idea ultimately served as the impetus for e-gel films, which were conceived during my efforts to expound upon his electrogelation technique.

Last, but certainly not least, there is Fio. In the best way possible, Fio Omenetto has always demanded more, challenging me and identifying ways in which I might develop into a more effective scientist. Often, this was not a comfortable process yet it remained a responsibility that he took very seriously, and from which I grew appreciably. For that, I am truly grateful. Fio's sense of creativity and uncompromising standard for quantitative detail are qualities that I can only hope to emulate. As I leave Tufts, I know that his example is one that will endure timelessly with me, as will my pride for having been a part of his lab.

TABLE OF CONTENTS

LIST OF TABLES

LIST OF FIGURES

1 INTRODUCTION

i. Why silk?

Silk has long been admired as a unique material. Produced by numerous insect larvae and webspinners, silk derived from the silkworm, *Bombyx mori*, in particular is regarded as a prized fiber, known for its strength and luster. As well, it is available in abundance, with over 100,000 metric tons produced annually.[1] Its main constituent, silk fibroin, is an FDA-approval biomaterial,[2] commonly used as medical sutures, and well-established for its mechanical strength, biocompatibility and biodegradability.

More recently, the value of silk has been extended appreciably through its solubilization and subsequent reformation into materials including films, fibers gels, foams, tissue engineering scaffolds, microspheres and nanoparticles.[3-17] The use of liquid silk, realized through relatively simple processing techniques, allows for the creation of nanopatterned surfaces and easy functionalization through the direct addition of chemical or biological agents, serving as the basis of a host of new opportunities in drug delivery and sensing.[18-21]

ii. Project Origins

The work presented in this thesis reflects the unpredictable nature of research. Both components of this effort were borne independently from a project with a

distinctly different goal: that of developing a biomimetic process to spin fiber from regenerated silk solution, and to use this fiber for optical waveguiding.

Along the way, I ventured into the world of sericulture in an effort to understand how the silkworm converts the silk dope stored in its middle gland into a solid fiber with remarkable properties. During that study, I learned a great deal about silkworm anatomy and physiology, as well as the intrinsic behavioral patterns that carry silkworms through their spinning process. Amongst my observations, I noticed how the silkworm is reliant upon its surroundings to spin a cocoon in its innate fashion. This is what led me to make silk mats, by manipulating the geometry of the local environment to influence silkworm spinning.

In considering applications for which mats could prove useful, I thought about dressings for wound healing. Drug-eluting silk mats, when properly degummed, might be useful not only for topical clinical applications but for implantation ones as well. Spurred by this idea, I tried to modify the food that silkworms ate, incorporating chemical additives into their mulberry leaf diet, with the hope of possibly seeing these molecules expressed within the resultant silk.

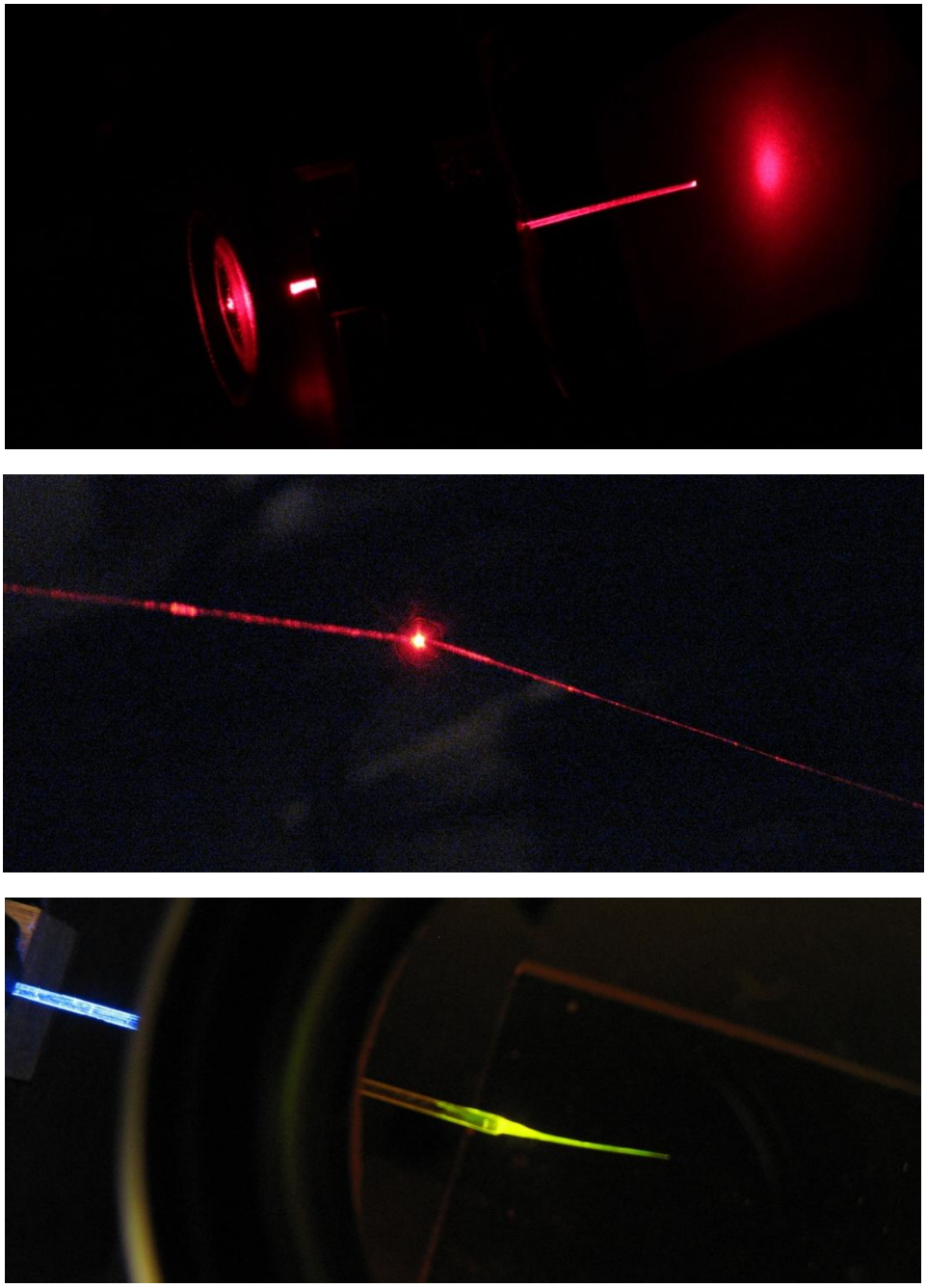

Figure 1. Samples of silk fibers shown guiding light: **a)** 632 nm HeNe laser light in silkworm gut, a fiber made by stretching a segment of silk gland; **b)** HeNe light coupled into single mode silica fiber and continuing into silk fiber made from regenerated silk fibroin solution; **c)** Blue (475 nm) light coupled into a silica multimode fiber and continuing into fiber made from regenerated silk fibroin solution doped with green fluorescent protein (GFP). Silk segment is viewed through a 550 nm long pass filter to reject blue excitation light.

An entirely different approach to making silk fibers was introduced to me by Gary Leisk and Tim Lo, who were the first to pursue the electrogelation of silk.[22] By placing two electrodes into silk solution and applying a current, one can generate a silk gel that develops around the positive electrode, the anode. Through subsequent temperature manipulations, this silk can be made amenable to drawing, leading to appreciable lengths of somewhat brittle silk fiber. At some point, out of pure curiosity, I wondered what might happen if we reformed the anode into the shape of a ring. Would gel form preferentially within the ring itself? Quickly, it became clear that it does, with far greater preference than I had originally expected. This served as the basis of e-gel films, named so to recognize their formation via the electrogelation process.

2 BACKGROUND

i. Silkworm Anatomy, Physiology and Life Cycle

The life cycle of the *Bombyx mori* silkworm begins as one of many fertilized eggs laid at once by an adult moth. Once the egg hatches, the resulting larva grows appreciably over the course of a month, from one millimeter in length to approximately 6-8 centimeters, by feeding on a diet of mulberry leaves. Over this period, the silkworm proceeds through 5 instars, shedding its skin (molting) 4 times. With its growth, the silkworm produces and stores an increasing supply of silk in its gland, which is subsequently used to spin a cocoon around itself, a continuous fiber that is on the order of 1 kilometer.[23] Inside the cocoon, the caterpillar changes into a pupa and then a moth, a process that takes 2 weeks. Subsequently, the resulting moth secretes cocoonases that allow it to escape from its cocoon.[24-26] The moth, however, has a life that is very short-lived. Possessing no mouth, it is unable to eat. Moreover, though it has wings, it can not fly. With a lifespan of approximately five days, its only need is to mate, thereby contributing to the next generation of fertilized eggs, and completing its life cycle. The frequency of this process is primarily a function of the voltinism of the silkworm breed; univoltine races produce only one generation per year. Multivoltine races can create up to seven generations in one year, though the quality of their silk is relatively poor.[27, 28]

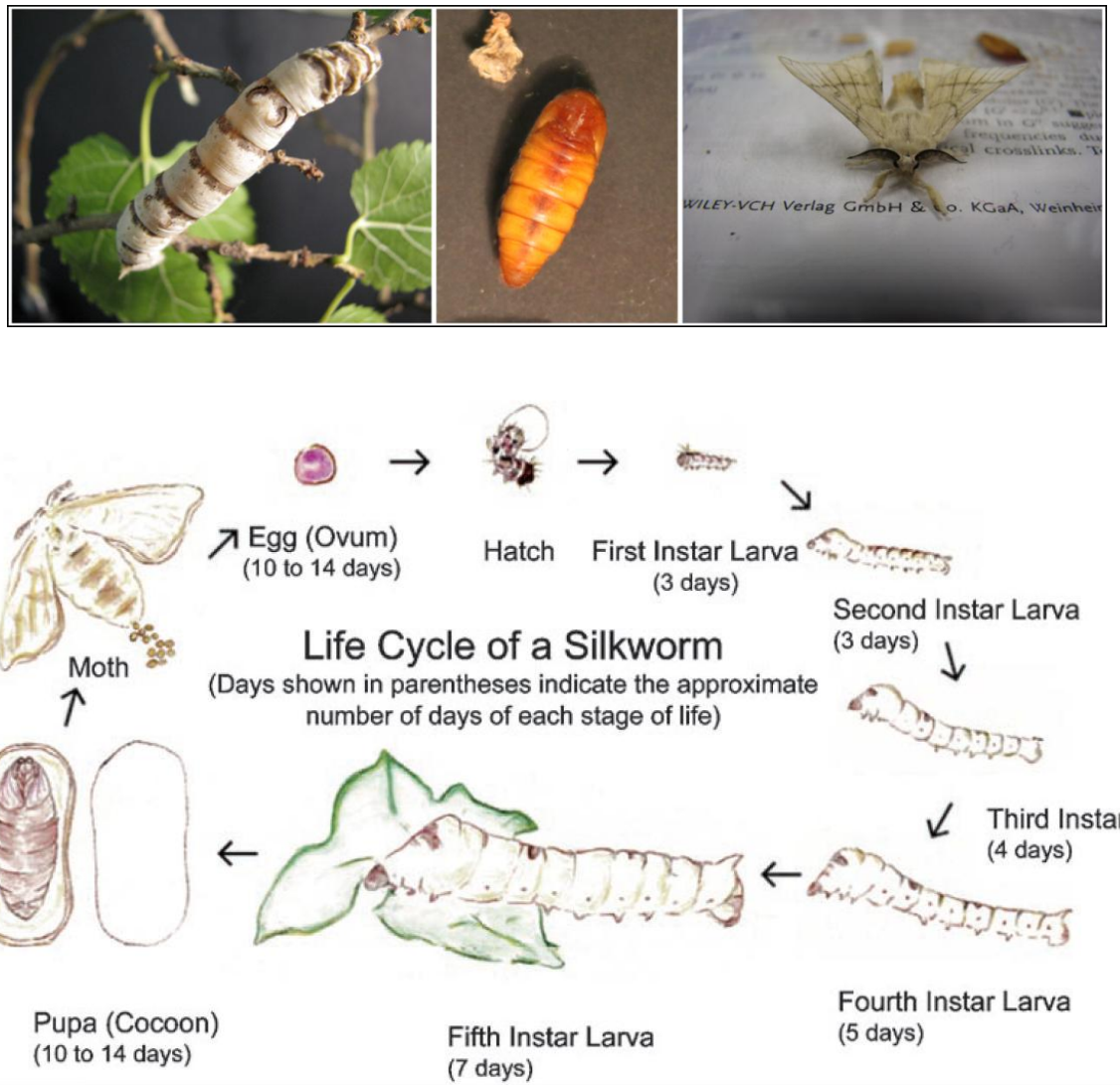

Figure 2. Top: photographs of silkworm 1) as a larva; 2) as a pupa; 3) as a moth. Bottom: Graphic of silkworm life cycle[27]

Our focus rests exclusively on the larval stage, where silk production occurs. The larval body is comprised of three main sections: the head, thorax and abdomen. Not surprisingly, its head is the most complex of these regions. It possesses two

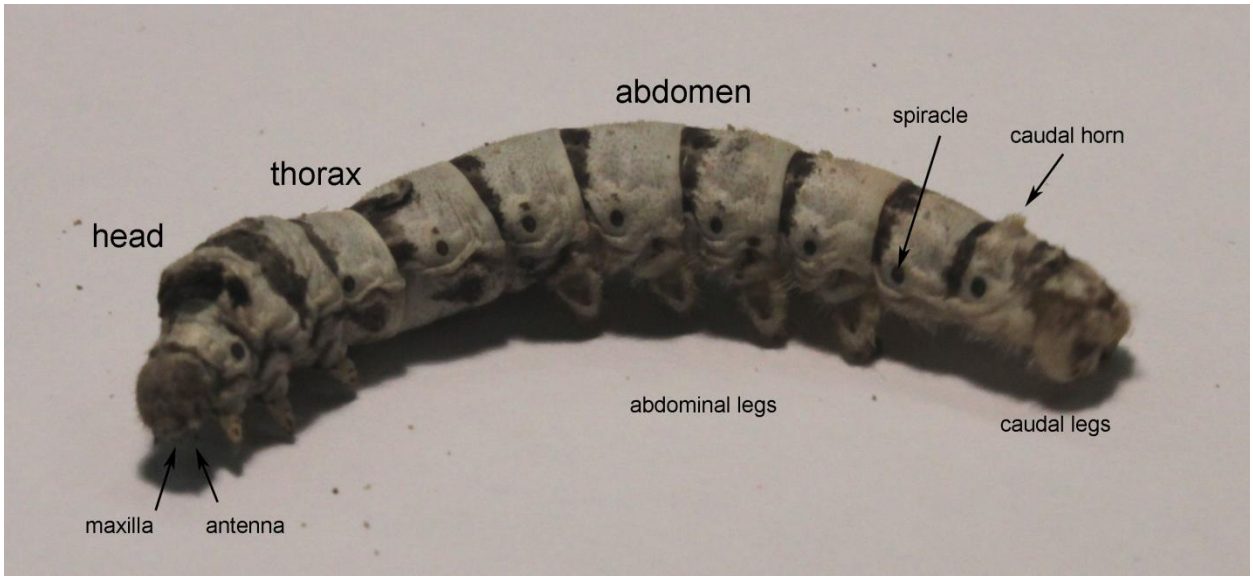

Figure 3. External silkworm anatomy

pair of ganglia: its brain as well the sub-esophageal ganglia, which control all nervous actions as well as the secretion of multiple hormones. The head also contains numerous sensory receptors on its antennae and maxillae, including photoreceptors called ocelli, olfactory and gustatory receptors for smell and taste, and tactile mechanoreceptors for a sense of touch. In addition, the spinneret, through which silk fiber emerges during spinning, is found within the labium (lower lip.) The thorax, most notably, contains three pairs of legs that carry sharp claws, useful for grabbing and holding mulberry leaves while feeding. The abdomen contains four pairs of abdominal legs, as well as a more distal set of caudal legs; together, these control much of the caterpillar's motion. Fittingly, this region also contains most of the muscles, both skeletal and visceral, that allow not

only for locomotion, but for contraction of the digestive tract and the silk glands to direct the flow of the fluids within. The abdomen also in where most of the silkworm's spiracles are found, through which respiration is conducted.

ii. How the Silkworm Spins

The silkworm possesses one pair of bilateral silk glands. Each gland works independently to produce a silk fiber called a brin, and the two brins are combined into on composite fiber immediately before silk emerges from the spinneret.

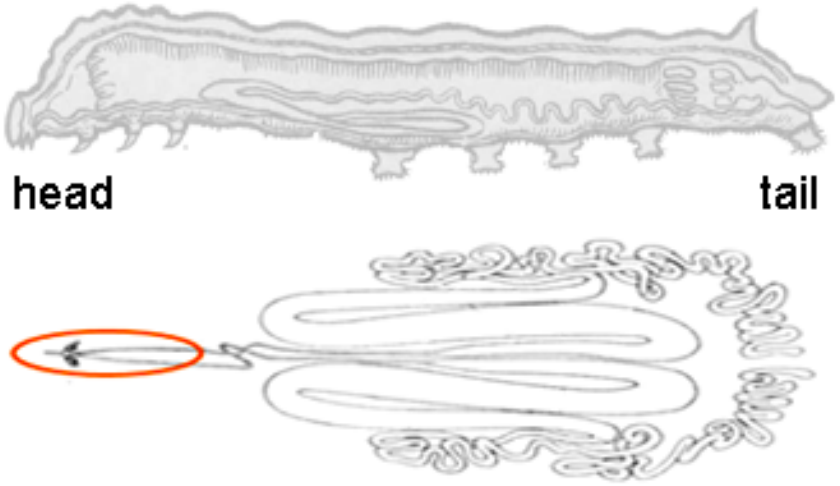

Figure 4. Depiction of silkworm glands. Fibroin is produced in the thin, circuitous posterior segments and then stored in the larger middle gland. Subsequently, it is passed through the anterior segments, where the glands are combined and the silk dope emerges through a spinneret in its head as a solid fiber. Filippi's gland (F), circled in orange, plays a role that to date remains unclear. [29, 30]

As shown in **Figure 4**, each gland varies markedly along its length, from its narrow but long posterior segment, where fibroin is initially produced, to the middle gland, where silk is stored as a fluid called dope, to the anterior segment, where silk is drawn down into a solid fiber. Along the way, layers of sericin proteins are secreted that coat each brin, acting as glues. In total, the sericin allows the brins to be held together, as shown in **Figure 5,** and keeps the resulting cocoon from unraveling.

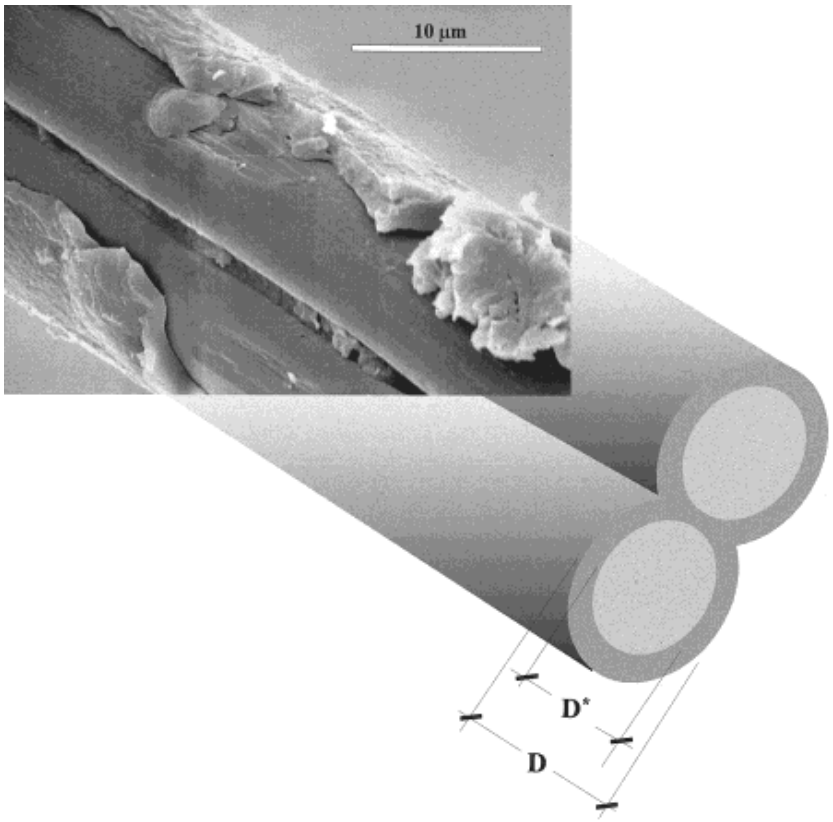

Figure 5. Bave silk is comprised of two brins, one for each of the silk glands. Fibroin, the main constituent of these fibers, is coated with a layer of sericin proteins, which can be removed through a process called degumming.[31]

At present, our understanding of how the silkworm converts silk dope into a solid fiber remains incomplete.[32] As silk dope progresses towards the spigot, four particular physical changes have been highlighted in the literature:

1. An increase in fibroin concentration[32-36]
2. A 100-fold increase in acidity, with pH dropping from 6.9 to 4.8-4.9 [37-39]
3. An increase in shear stresses, owing to a tapering in the gland.[35,40-50]
4. Changes in ion content[39,51-55]

This combination of events induces conformational changes within the silk molecule that lead to bulk solidification. Yet for all that is known about the silk spinning process, nobody has been able to reproduce it experimentally, at least in a manner that could truly be deemed biomimetic. Most efforts to generate silk fiber have been conducted using wet spinning[56-64] where silk is extruded into a bath containing a solvent that stimulates coagulation, or electrospinning[65-67] where a high voltage is applied to a silk droplet, creating a charged liquid jet that forms a fiber as it dries.

iii. Production of Regenerated Silk Fibroin Solution

In the production of regenerated silk fibroin solution, silk cocoons are exposed to a series of chemical treatments that end in the realization of liquid silk, as shown in **Figure 6**. Initially, sericin proteins are separated from the silk fibers

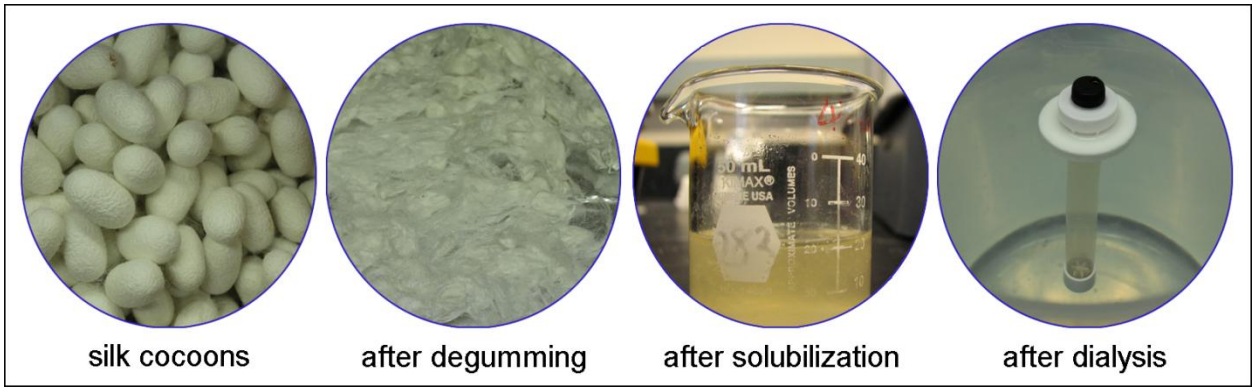

Figure 6. Steps for the realization of regenerated silk fibroin solution, shown by their resulting products.

themselves, which are comprised of fibroin, through a process known as degumming. In this, silk cocoon fragments are plunged into a boiling sodium carbonate solution. The high-temperature, alkaline treatment can remove sericin almost completely in as little as 5 minutes. The degummed fibers are then rinsed multiple times in ultrapure milli-Q water, to remove residual sericin, before being left to dry. The remaining dried fibroin is approximately 30% lighter than the original cocoon segments.

Fibroin is solubilized through the addition of a chaotropic salt such as lithium bromide, resulting in a sticky fluid with a yellow hue. This reaction is accelerated by heat, so it customarily is conducted inside an oven at 60°C. For silk that has been degummed via a 60 minute boil, solubilization requires 4 hours. An inverse relationship exists between boiling time and solubilization time, however. Silk that is degummed via a 10 minute boil requires 16 hours for solubilization.

Beyond this aforementioned relationship, degumming time also influences the physical properties of the resulting silk solution.[68-76] Longer boiling times result in increased fibroin degradation and consequently, smaller and more random silk fragments from once-intact fibroin molecules. From personal observation, this translates into a solution with a much lower viscosity, a broader spectrum of (lower) molecular weights as measured by SDS-PAGE, and a broader spectrum of isoelectric points (pI) as measured by isoelectric focusing (IEF).

After solubilization, silk solution consists predominantly of salt, which must be removed to isolate the liquid silk. This is realized through dialysis against milli-Q water, with multiple changes over the course of three days to maintain favorable chemical gradients for the passive transport of salt ions across the dialysis membrane. Moreover, the choice of dialysis membrane is significant. Dialysis can be accelerated somewhat through use of a membrane whose geometry maximizes the surface area to volume ratio; thus, a long, relatively thin tube is a better choice than conventional dialysis cassettes. Moreover, the use of more rigid membranes, which do not swell appreciably, reduces the extent to which the remaining silk solution is diluted by limiting the inflow from the dialysate into the silk solution.

iv. Electrogelation

Electrogelation is a process by which silk gel, called an e-gel, is created through the application of electrical current within a regenerated silk fibroin solution. Typically, this work is conducted using a power supply under constant voltage, using a potential difference between 5-25V. Since regenerated silk solution is comprised predominantly of water, the reaction is in large part governed by the threshold value for water electrolysis, which is 1.23V. As well, electrode selection is important, requiring metals that interact minimally with the surrounding solution, such as gold or platinum. Copper electrodes should be avoided as they release copper ions into solution and confer a blue-green tinge to the resulting e-gel.

Figure 7. Silk e-gel mass on a platinum electrode

3 E-GEL FILMS

i. Introduction

Current methods to produce silk films include casting and spin coating. I introduce a new method for the fabrication of silk films: electrogelation. By using a closed-loop anode, the controlled application of electrical current to regenerated silk fibroin (RSF) solution yields a silk gel which, upon drying, forms an optically transparent film. This technique allows for the rapid production of freestanding, mechanically robust thin films with desirable characteristics that include exceptionally low surface roughness, curved geometries, and thicknesses into the nanoscale.

Recently it has been established that RSF solution, derived from Bombyx mori silkworms, responds to direct current (DC) electrical stimulation by aggregating around the anode and forming a gel, called an e-gel to specify the method of its formation.[22,78,79] A common thread in preceding works is the use of simple electrodes that are rod-like in their geometry. I expound upon this 1-D approach to show that configuration of the positive electrode into a closed loop leads to the formation of silk films that are circumscribed by the loop itself. Moreover, in contrast to other electrodeposition studies, both with silk and other biopolymers, the resulting e-gel films are freestanding, possessing no underlying surface and

supported only at the films' edges.[22,77-85] In the simplest case, the loop lies within a 2-D plane, and a flat circular film is produced. In addition, through manipulation of the loop, a number of 3-D topologies can be realized.

ii. Methods: Fabrication

Regenerated silk fibroin (RSF) solution was produced through slight modifications to the standard process.[22,77,87] Degumming time within a 0.02 M sodium carbonate solution was limited to a 10 minute boil, shorter than in preceding papers discussing the e-gel process, to minimize fibroin protein degradation.[22, 77] Correspondingly, fibroin was solubilized in 9.3M lithium bromide for 16 hours in a 60˚C oven to allow for more complete unfolding of the comparatively longer fibroin chains. The chaotropic salt was subsequently removed through dialysis (3.5 kDa MWCO) against Milli-Q water for a total of 72 hours, yielding an 8% (w/v) silk solution. The resulting liquid was then purified by centrifugation at 8,800 rpm over two 25-minute long periods, with the temperature held constant at 4˚C.

Ring-shaped electrodes were produced from a selection of gold (0.2 mm diameter) and gold-plated (0.6, 0.8 and 1.0 mm diameter) wires (Alfa Aesar and Paramount Wire Company). To assure reproducibility, each anode was created by hand by twisting the wire around rigid plastic cylinders of known diameter, ranging from 7 to 20 mm. Meanwhile, the cathode remained a straight segment of

gold wire. For film fabrication, 2 mL of silk solution were deposited into polystyrene tubes prior to introduction of the ring anode and straight cathode. Current was delivered to the solution through a power supply at 5, 10 or 25V, constant voltage, for durations between 0.5-10 minutes. The positive electrode, circumscribing a silk film, was subsequently removed and allowed to air dry. Changes in silk concentration between the e-gel film and the surrounding solution were measured by comparing the wet and dry masses of samples collected following electrical stimulation.

The electrolysis of water is believed to play a critical role in the electrogelation process. To examine the temporospatial evolution of pH gradients within silk solution exposed to DC current, 5 μL of methyl red indicator dye (Riedel-de-Haën) was added to 2 mL of silk solution. Methyl red is an azo dye that appears red below pH 4.4 and yellow above pH 6.2. The initial RSF pH, measured by short-range pH paper (Micro Essential Lab, Hydrion) was 6.5. Gold-plated rods, 0.6 mm in diameter, were used as electrodes at a separation distance of 5 mm. Video was recorded for 10 minutes at 10V, constant voltage (Mastech, HY3005D-3 DC).

iii. Fabrication Results

E-gel films with unique geometries were produced as shown in **Figure 8**,

enabling silk films with topologies that can not be realized otherwise through existing silk film fabrication methods. The applications for this approach include biosensors and drug delivery devices with unusual geometries that can be molded to fit conformally upon target organs, as well as customized patient-specific tissue engineered scaffolds for curved but stratified tissue architectures. These ideas serve to complement a recent paper that introduced initially flat silk films that conformed to the brain through wetting. However, acceptable conformation to the underlying tissue geometry was only apparent for films less than 7 microns thick.[22]

Figure 8. A selection of anode geometries reflect the ability of this process to create silk films from **(a)** a simple circled-shaped sheet to non-planar topologies including **(b)** an 'S' and **(c)** a saddle point.

The mechanism of e-gel assembly was shown to be driven by a localized decrease in solution pH, a byproduct of the electrolysis of water.[77, 78] The electrical current required is small, less than 1 mA. While a current is applied, the local pH in the vicinity of the anode decreases, and oxygen gas is released by the following

reaction:

$$H_2O \rightarrow \frac{1}{2}O_2 + 2H^+ + 2e^- \quad (1)$$

Conversely, fluid in the vicinity of the cathode experiences an increase in pH and hydrogen bubbles are released as follows:

$$2H_2O + 2e^- \rightarrow 2OH^- + H_2 \quad (2)$$

Figure 9 depicts the evolution of pH gradients within an RSF sample as shown through the use of methyl red, an indicator dye that is colorless for 4.4 < pH < 6.2. A solution more acidic than pH 4.4 appears red, while one that is more basic than pH 6.2 appears yellow. Using short-range pH paper, the initial pH of silk solution was measured as 6.5. With increasing time, acidification of the local environment around the anode is evident and expanding.

Local changes in pH induce conformational changes within the silk molecule, as shown in **Figure 10**.[33, 88, 89] A number of papers examining the gelation of silk solution have shown that a pH of approximately 5 serves as a critical threshold, below which silk solution will gel rapidly.[77, 86, 90] This also is consistent with studies of silkworm physiology, which have found that the transition of silkworm silk solution from dope in the gland to a spinnable gel occurs at pH 4.8.[37, 38]

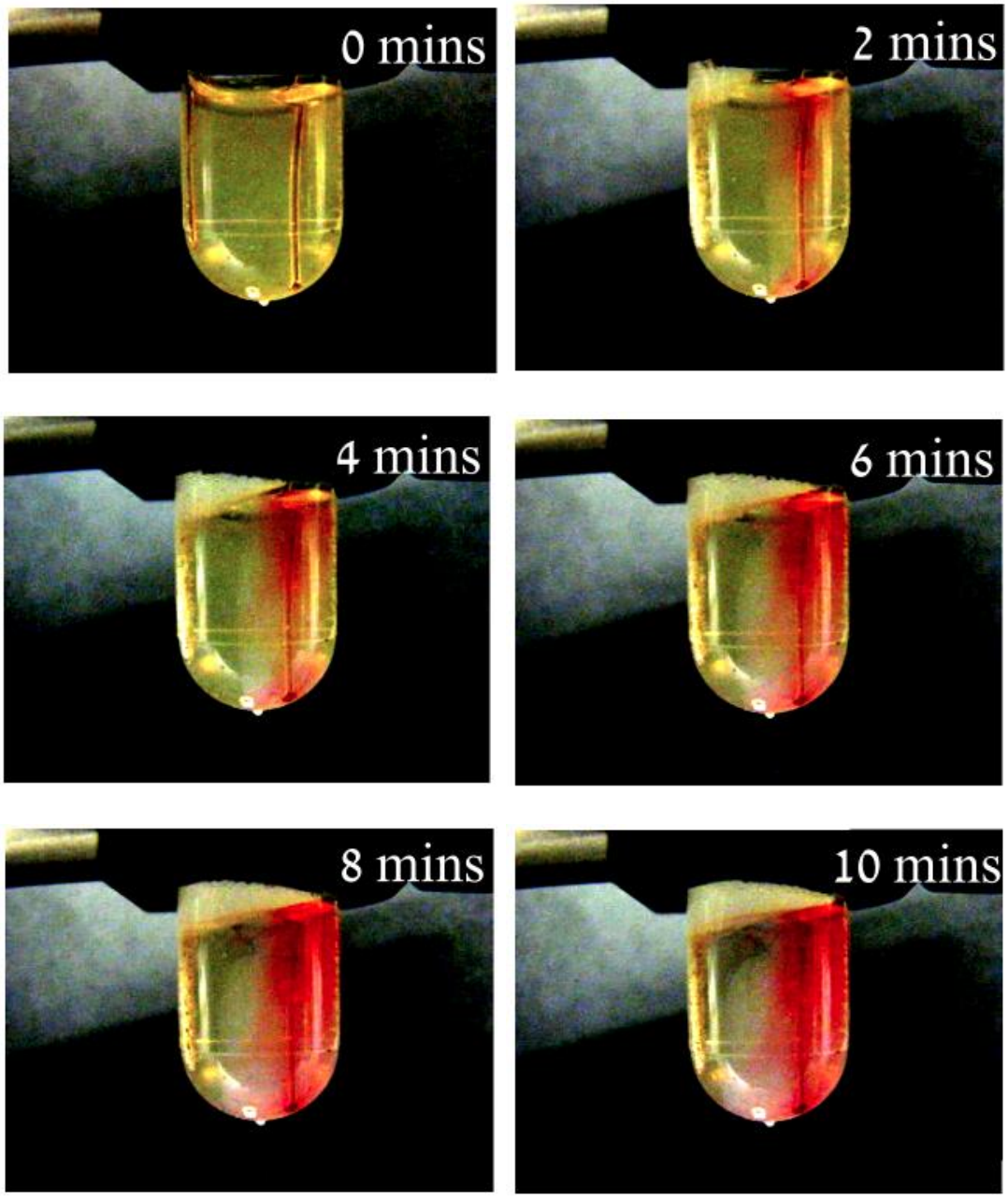

Figure 9. Silk e-gel formation parallels pH gradient evolution. Using a DC power supply, 10V (constant voltage) were applied to a silk solution (initial pH: 6.5) containing methyl red indicator dye. With increasing time, fluid around the anode (positive electrode, at right) experiences a significant decrease in pH and a growing aggregate of e-gel mass is apparent.

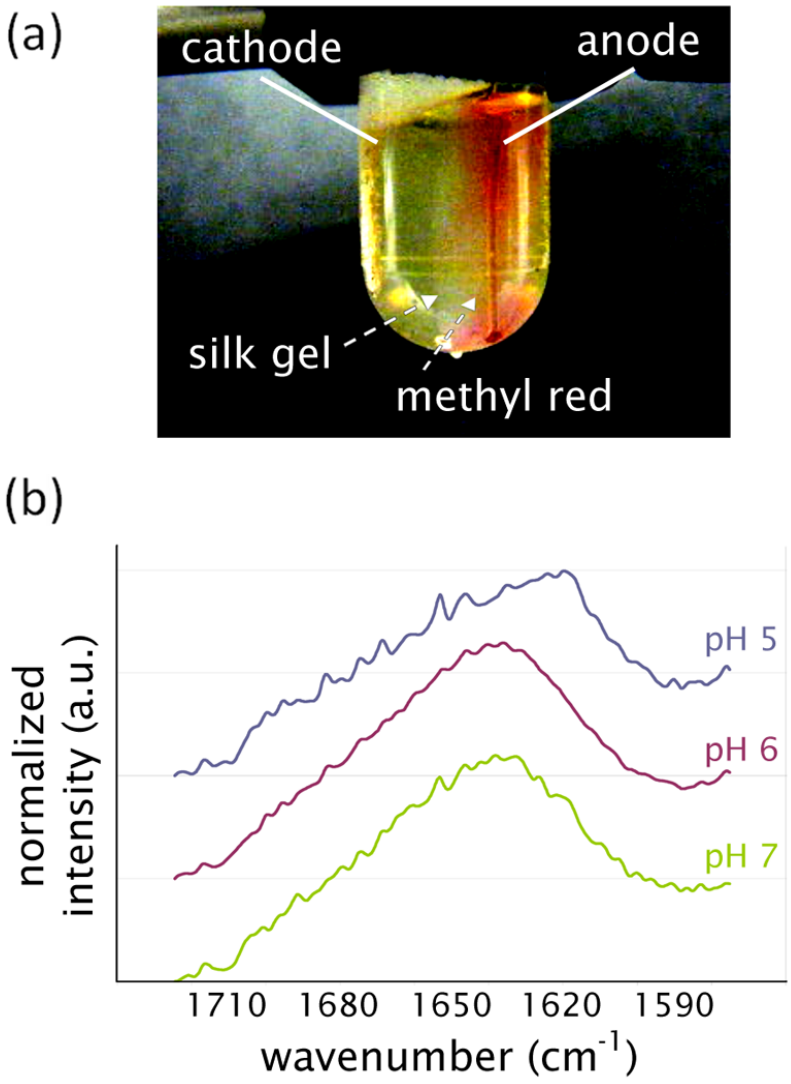

Figure 10. (a) The silk gel, visible in white, leads the methyl red front, corresponding to thresholds for these events, pH 5.0 and 4.4, respectively. **(b)** Increasing acidity produces conformational changes within the protein, as shown by FTIR. This is particularly evident within the 1616-1637 cm^{-1} region, representing enhanced beta-sheet content.

The role of electric charge in the process is significant as well. Silk molecules are negatively charged, and throughout the literature, experimental measurements of the isoelectric point (pI) of silk fibroin fall between 3.6-4.2, well below the initial pH of RSF solution.[90-93] Electrical stimuli thus promote the migration of silk molecules towards the positive electrode, a behavior validated by measured increases in silk concentration within the e-gel mass, relative to the surrounding solution. Independently-evolving pH gradients coincide with this behavior, as the anodic environment gradually approaches the threshold for silk gel formation.

E-gel films allow for the production of curved films across a range of thicknesses. **Figure 11** shows cross-sectional scanning electron microscope (SEM) images of films ranging from those tens of microns thick to thin films with submicron thickness. Film thickness can be controlled by numerous factors including wire gauge, voltage, silk concentration and exposure time. Thin films are of particular interest as they lend to applications in photonics and optoelectronics.[95, 96] Further, by comparison with other silk film fabrication methods, the electroglelation process allows for more facile fabrication and yields thin films that are easier to manipulate.[97]

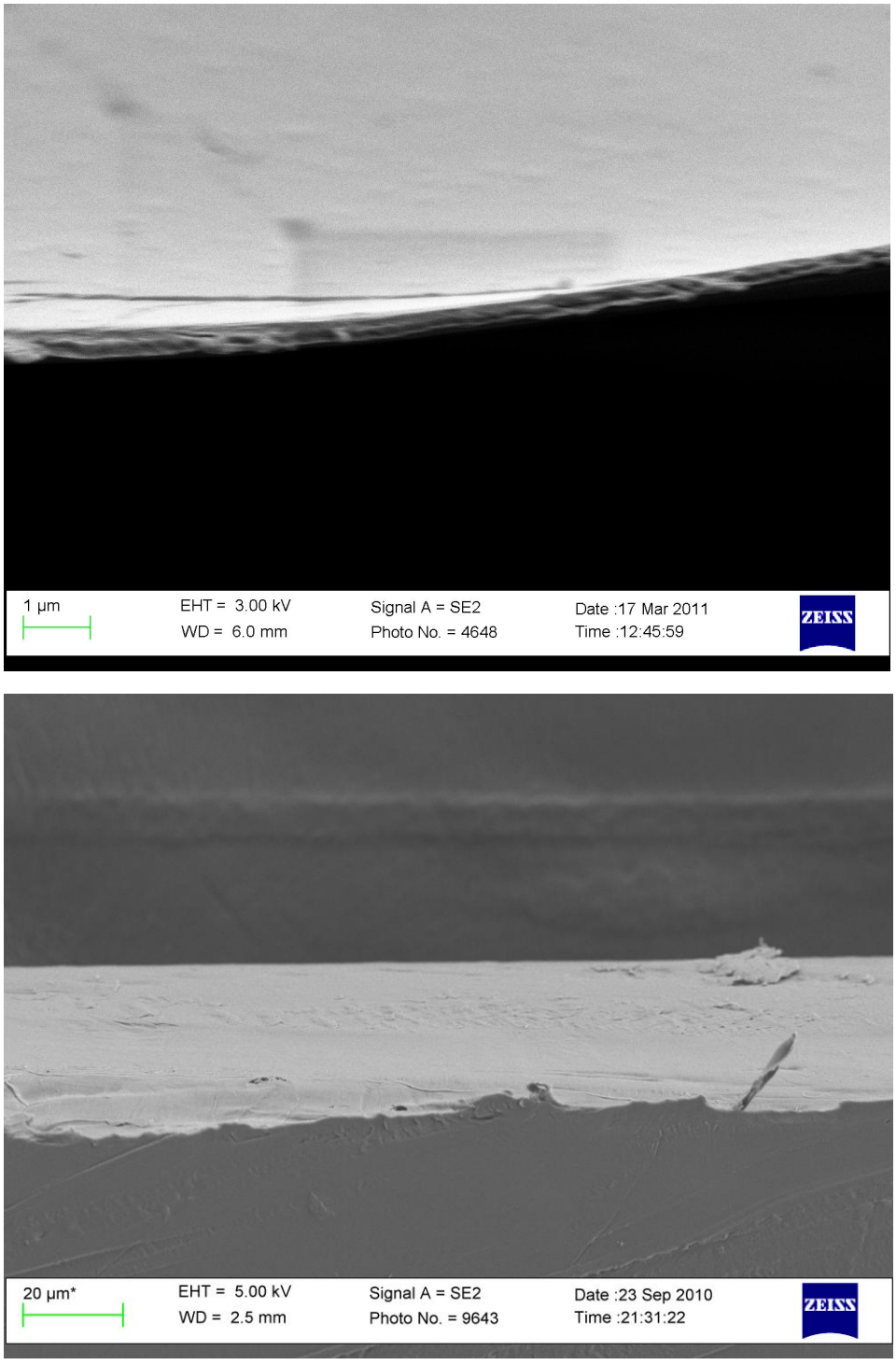

Figure 11. E-gel films can be made across a range of thicknesses.
Top: Thin film approximately 500 nm thick
Bottom: Film thickness of approximately 50 µm.

iv. Discussion

The e-gel film process represents a simple, inexpensive and easily portable method for the generation of freestanding biopolymeric thin films and is summarized in a flowchart in **Figure 12**. Use of a ring-shaped anode forces the initial gel growth to form as a sheet that is confined to the plane of the electrode and circumscribed by the ring itself. Only after that space is occupied will silk gel develop above and below the initial plane and around the wire. This result is entirely different than what is observed in an incomplete loop, such as one interrupted by a cut, where gel formation envelops the wire uniformly both in and outside of the loop and no film is produced. The difference between these two events reflects the uniqueness of the closed loop result and suggests the role that electric field distribution may play in the e-gel film process, promoting an almost exclusive aggregation of silk mass within the plane of the ring.

A significant number of variables exists that affect the ease with which e-gel films can be produced. **Table 1** considers those of the setup itself, examining the primary environmental variables that play a role in e-gel film formation. **Table 2,** on the other hand, considers key parameters influencing the amenability of silk solution to forming e-gel films.

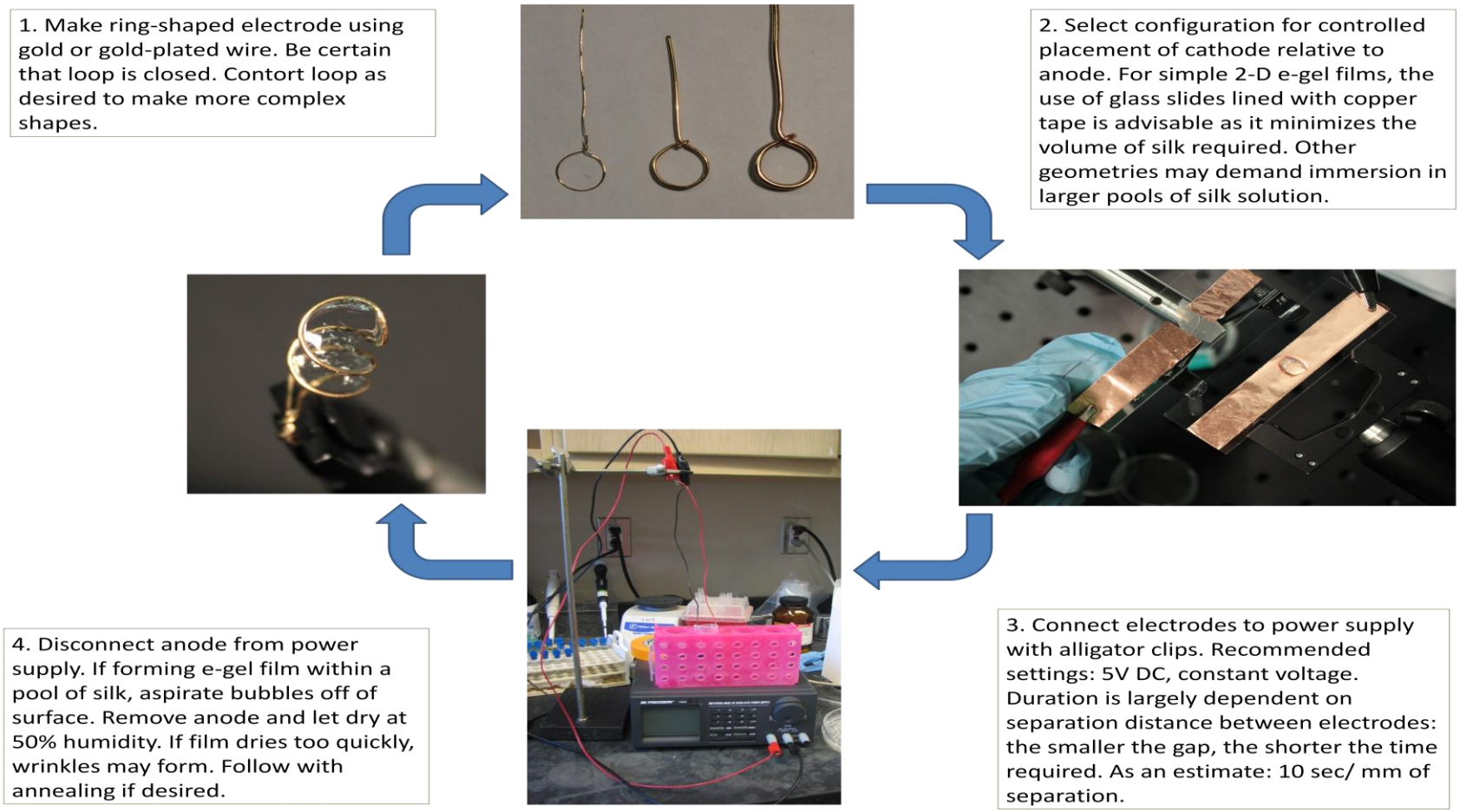

Figure 12. Flowchart describing the e-gel film fabrication process

Variable	***Effect***
Electrode material	Material resistivity dictates how easily charges can move at a fixed voltage
Electrode gauge	Wire cross-sectional area also influences current and electric field strength
Ring diameter	Larger ring leads to slower-forming film
Electrode separation	Decreasing separation distance accelerates film formation
Voltage/current	Higher values accelerate e-gel film generation but also lead to increased bubble formation
Exposure time	Longer time can lead to thicker films but also less uniform ones in cross section

Table 1. Roles of significant environmental variables on the e-gel film process.

Variable	***Effect***
Molecular weight	Less degraded silk responds far more favorably and more consistently than silk solutions produced via longer degumming times.
pH	The higher the starting pH, the longer the time for e-gel film formation
Concentration	Higher concentration accelerates film formation and can increase film thickness
Silk age	Increased (irreversible) beta-sheet content inhibits e-gel formation

Table 2. Roles of significant RSF solution variables on the e-gel film process.

Previous papers highlight the problematic role that bubble formation plays within the developing e-gel, as the gaseous products of water electroylsis. Electrode geometry is significant. With a rod-shaped anode, oxygen bubbles nucleate upon the electrode's surface and accumulate within the expanding gel, compromising mechanical stiffness and serving as an electrical insulator that retards continued gel formation.[22, 77, 78] At the cathode, hydrogen bubble nucleation takes place at a rate double that of anodic oxygen as per the overall electrolysis reaction:

$$2H_2O(l) \rightarrow 2H_2(g) + O_2(g) \quad (3)$$

Flat ring-shaped anodes avoid significant bubble interference during film formation, an effect that can be explained by geometry: while a film develops within the ring, the silk-metal interface on the outside of the ring does not experience any significant e-gel mass accumulation, allowing bubbles to escape without becoming entrapped within the forming gel. Moreover, the rate of bubble formation can be minimized by regulating electrical current within the solution.[78, 98] It is of note, however, that some three-dimensional configurations result in the entrapment of bubbles, as shown in **Figure 13**, though this effect can be minimized through the use of filters that capture or redirect bubbles away from the developing e-gel film.

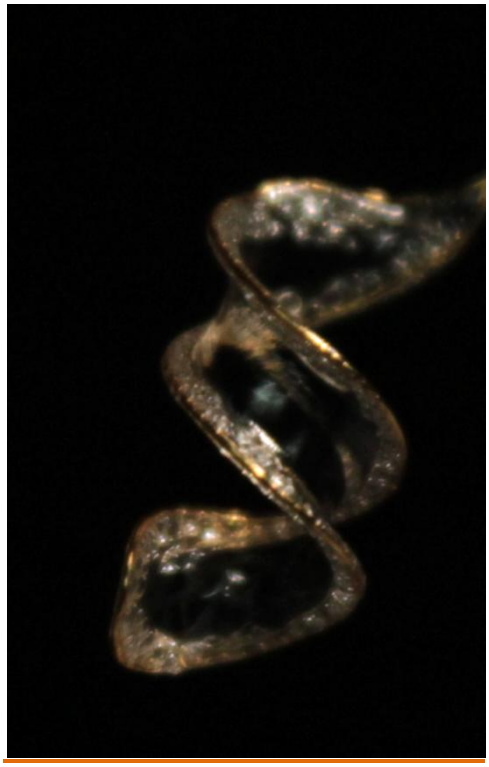

Figure 13. Helical e-gel film with bubbles visible around the electrode.

4 E-GEL FILM CHARACTERIZATION

i. Methods

E-gel films were studied using a host of analytical tools. SEM (Carl Zeiss, Ultra55) images were collected, after sputter coating (Cressington, 208HR) with a Pt/Pd target, using both InLens and secondary backscatter detectors. AFM (Veeco, Nanoscope III) images were recorded in air using Research Nanoscope software version 7.30 (Veeco). A 225 μm long silicon cantilever with a spring constant of 3 N/m was used in tapping mode. FTIR spectra were taken using an ATR probe, with subsequent background subtraction.

Optical transmission was measured in software (Ocean Optics, SpectraSuite) using a tungsten-halogen light source (Ocean Optics, LS1) and a visible-range spectrometer (Ocean Optics, USB2000) Refractive index was determined using a commercial refractometer (Metricon, 2010 M prism coupler).

ii. Characterization Results

Surfaces of e-gel films are extremely smooth, as shown in **Figures 14** and **15**. Multiple straight line topographical measurements taken across a 10 μm x 10 μm film section with an atomic force microscope (AFM) yielded root-mean-squared (RMS) values between 4- 6 Å. On a larger scale, SEM images of a film section with dimensions of the order of a millimeter showed no detectable surface defects. These results are in contrast with results from alternating current (AC)

experiments, where the mean roughness was two orders of magnitude higher, suggesting that silk molecules may align themselves in response to the DC field.[99]

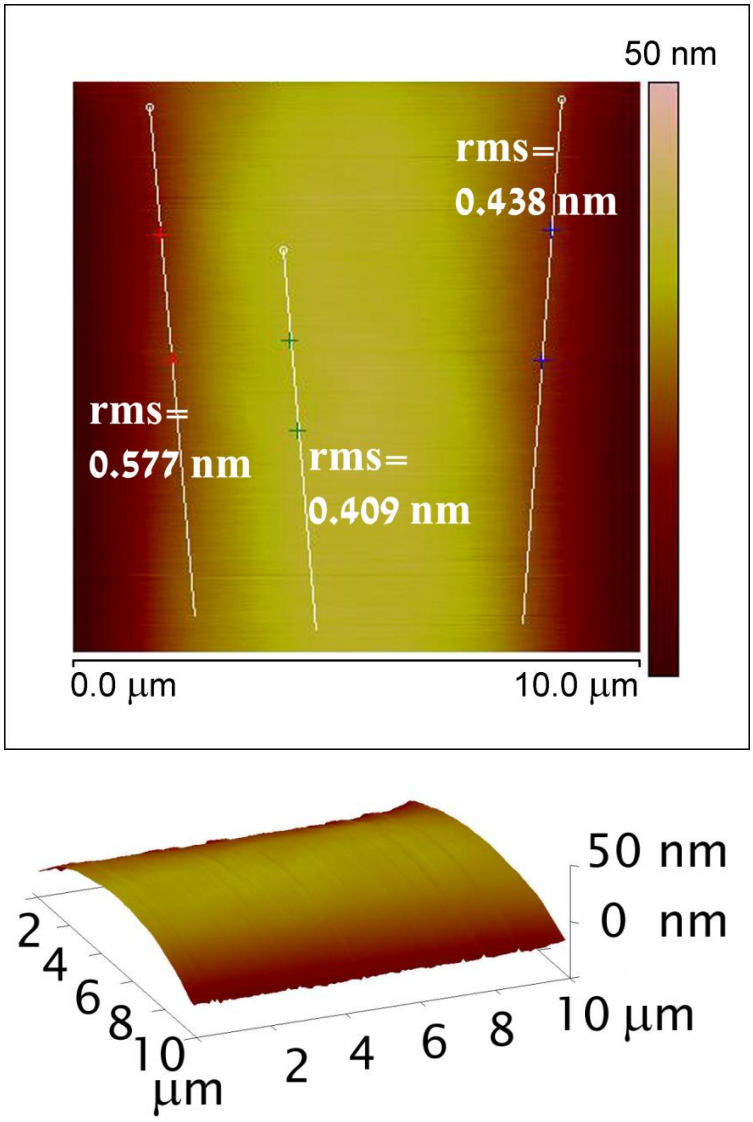

Figure 14. AFM images of a sample area 10 µm by 10 µm, show minimal surface roughness. RMS values of 4-6Å were seen along sample paths 1.5-2.5 µm in length, drawn orthogonal to the visible variations from adjacent horizontal line scans.

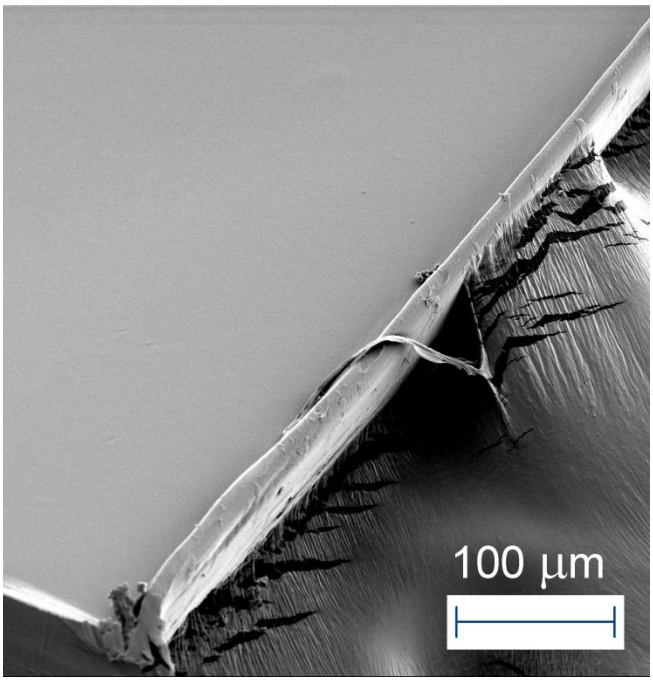

Figure 15. On a larger scale, e-gel films maintain very low surface roughness, making them desirable for optical transmission. An SEM image of an e-gel film segment illustrates gross smoothness of the e-gel film face across a larger area. The edge roughness is due to manual cutting with a razor blade.

Silk films produced via electrogelation are optically transparent, with characteristics similar to those observed in silk films made by other methods. Spectroscopic measurement of optical transmission is in excess of 90% across the visible spectrum for films 20-30 μm thick, as shown in **Figure 16**, which compares favorably to previously reported results for cast silk films.[7, 17] In addition, refractive index measurements of $n = 1.54$ using a commercial refractometer showed little difference from previously published results employing other silk film fabrication techniques.[11, 17, 100]

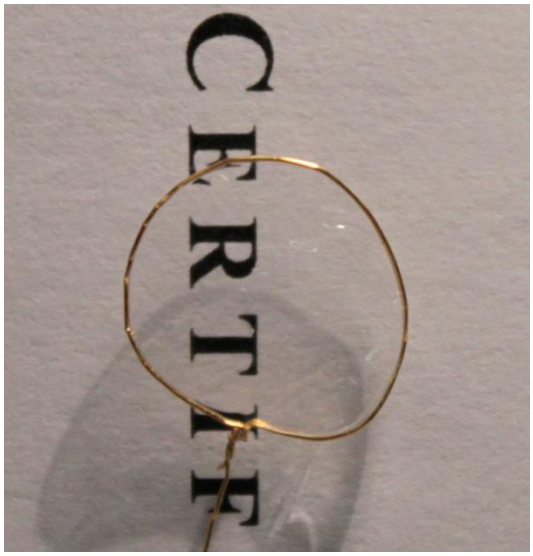

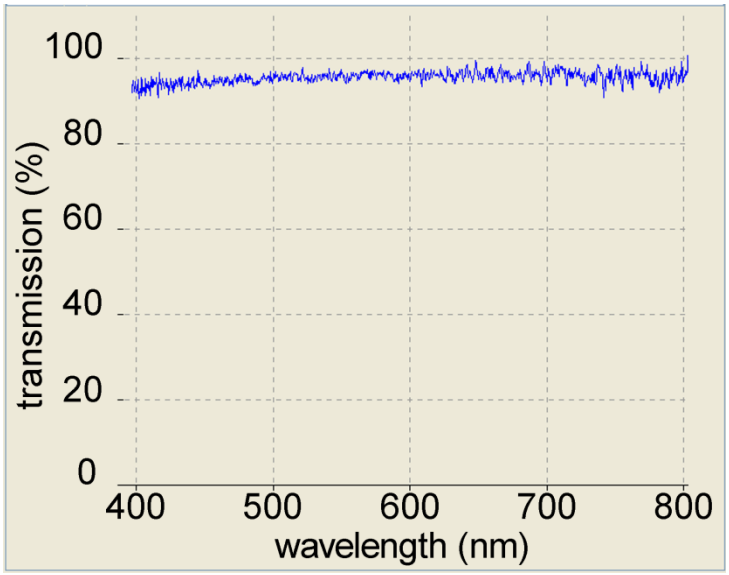

Figure 16. Silk e-gel film transparency is shown using a sample approximately 25 μm thick. The corresponding optical transmission spectrum agrees with the preceding physical example.

iii. Conclusion

Previously, electrogelation was noted for its potential to generate biocompatible adhesive silk as well as for its ability to serve as a complementary process to hydrogels and gels formed via sonication.[86, 93, 100-102] Here, electrogelation with a closed-loop anode is shown to be a rapid, novel approach for generating silk films that are exceptionally smooth. Further, manipulation of the electrode can confer curvature to the resulting films, something unattainable via alternative methods. Fine control of the fabrication process has shown the capability to generate a range of film thicknesses from tens of microns to hundreds of nanometers, creating interesting opportunities in a number of fields spanning photonics and optoelectronics to biosensing, drug delivery and tissue engineering.

5 NATURAL SILK MATS

i. Introduction/ Motivation

With an initial goal of developing a biomimetic process to produce silk fiber, I raised hundreds of silkworms and studied their spinning process. This perspective made one particular behavioral element apparent: that silkworms draw their fiber by affixing a droplet of liquid silk onto a surface and then pulling. This simple observation contrasts an approach seen in a preponderance of papers in the literature, mainly employing wet spinning, that attempt to replicate the spinning process artificially by modeling it as extrusion-based.[56-64] Rather, it is likely that a fiber emerges through the silkworm spinneret owing to the shear stresses imposed on the dope through pulling, thereby converting this fluid into a solid. [40-50]

The importance of this discrepancy is significant in considering the role of anchor points. Prior to spinning its cocoon, the silkworm erects a scaffold in which the cocoon is encapsulated. This precedes the 'figure-8' motion seen later in cocoon spinning.[104, 105] During the scaffold building phase, the silkworm creates long straight fibers that are attached to points in the surrounding environment, such as branches. When interconnected, these fibers suspend the cocoon in its desired position. The end points of these longitudinal fibers are known as anchor points and must help to support the weight of the cocoon and its silkworm. By necessity, the anchor points are adhesive. Liquid silk is adhesive while solid fibers are not.

Thus, it is inferred that the silkworm ejects some combination of both liquid and solid silk to serve multiple requirements, those of adhesion and mechanical strength.

In thinking about anchor points, a series of seemingly logical questions arose: after placing an anchor point, how does the silkworm decide where to place the next ones in succession? How would the silkworm respond if we dictated its prospective anchor point sites through controlled manipulation of its local environment? Finally, how might the substrate material available for anchor points influence the spinning process? These questions prompted the study presented herein.

ii. Initial Methods/Strategies

Bombyx mori silkworms [Coastal Silkworms and Mulberry Farms] were raised either on a diet of fresh mulberry leaves or reconstituted mulberry chow, depending on the seasonal availability of fresh leaves from a tree on campus at Tufts. Silkworms were first raised as groups in large (150 mm diameter) petri dishes before being transferred to individual 100 mm diameter petri dishes as they entered their 5th instar.

As a silkworm approaches its time to spin, it exhibits a number of telltale signs. It stops eating and enters a wandering phase, where it periodically raises its head so

that the front half of its body is somewhat upright.[106, 107] Once this behavior manifests itself, or shortly thereafter when spinning had just begun, silkworms were placed on flat substrates that were either supported from underneath or suspended from above in manners that forced the silkworms to remain on the substrate upper surface. In the first iteration, a 12" by 12" acrylic sheet was used as well as a 4.5" by 6" Teflon one. Subsequently, a number of silkworms were placed on individual Teflon sheets, cut 3" x 3" in area, and mounted atop optical post holders using double-sided tape.

It was later posited that the absence of a vertical dimension may not be a requirement for mats to be spun instead of cocoons: how might the silkworm adapt in situations where a relatively minor height exists, which offers the opportunity to establish anchor points, albeit suboptimal ones? Experiments were designed to establish whether a threshold height exists, below which mats will be formed and above which cocoons will be spun. Silkworms were left to spin inside the bowl of polystyrene Petri dishes, 10 cm in diameter and 12.5 mm in height as well as the accompanying lids, which were 7.5 mm in height. These heights were selected because they fall slightly above and below the thickness of the pupa that forms within the cocoon.

Building upon this understanding of anchor points, one additional question was asked: might it be possible to manipulate anchor point placement to generate

cocoons with interesting geometries, such as pyramids or triangular prisms? In the hope of creating a pyramidal-shaped cocoon, silkworms were placed atop a 3" x 3" Teflon sheet. A thin Teflon rod was suspended directly overhead, approximately 1" above each Teflon sheet, and the rod's bottom face was covered with double-sided copper tape. Thus, the prospective anchor points were limited to the cut faces around the perimeter of the Teflon sheet as well as the bottom face of the Teflon rod. Similarly, efforts at a triangular prism-shaped cocoon utilized a Teflon 90° elbow, where available sites for anchor points were limited to cut Teflon surfaces, comprising two parallel lines on opposite sides of the elbow.

iii. Results

Silkworms placed upon acrylic sheets, flat circular polystyrene dishes and square Teflon sheets demonstrated an ability to adapt to their surroundings; when constrained to two dimensions, the silkworms spun silk mats that conformed to the shape of the underlying substrate, as shown in **Figure 17**. On the acrylic and polystyrene surfaces, the entire mat area adhered to the underlying substrate. In contrast, mats spun atop Teflon only adhered at their edges. While the Teflon surface itself did not allow for any anchor points, the roughened edges where the Teflon was cut to size did. The unique behavior of this material often confounded the silkworms at first, leading them to fall off of the Teflon sheets, often multiple times. Each time, they were placed back atop the Teflon sheets, and silkworms adjusted to this environment progressively.

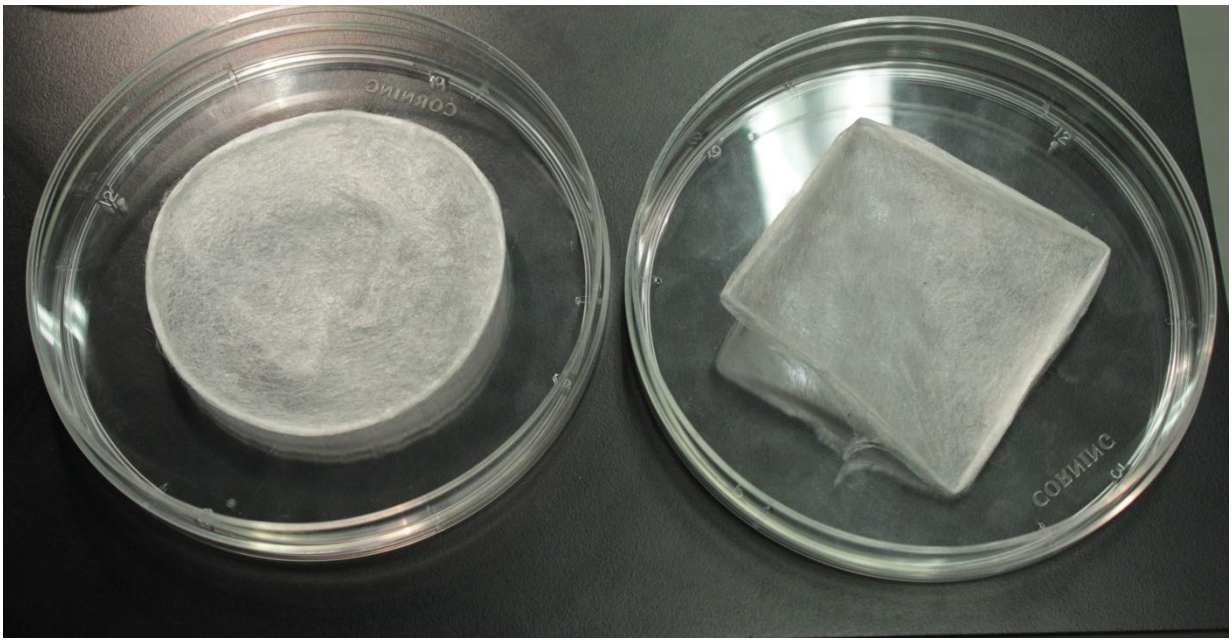

Figure 17. Natural silk mat samples. At left, a 10 cm diameter circle. At right, a square with 3" edges.

Upon the substrates with moderate surface area, including the 3" x 3" Teflon sheets and 10 cm diameter Petri dishes, the layer of silk that is deposited appears relatively uniform. Substrates with larger surface area however, such as the larger Teflon and acrylic sheets, were too large to allow for spinning across the entire surface. What was observed there reflected a somewhat different result, as the silk coverage was localized and non-uniform. Still, anchor points were evident, as shown in **Figure 18**. Silkworms have little choice but to exhaust their silk supply; it has been established previously that silkworms must empty their gland in order to proceed with their life cycle, and that they die if they do not. Upon exhausting

their supply of silk, silkworms continue about their life cycle despite lacking the conventional protection of the cocoon, morphing into pupae and then adult moths.

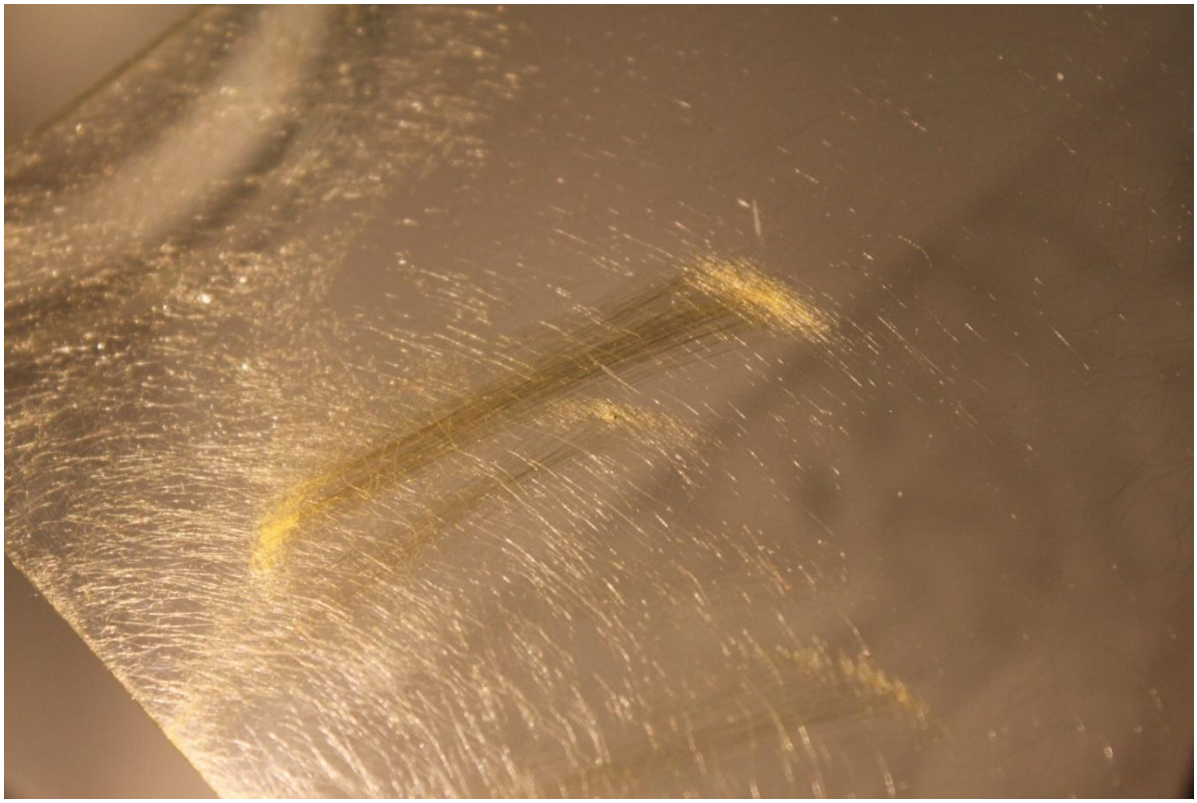

Figure 18. Silk spun atop a 12" square acrylic sheet. Bright yellow band reflects the silkworm's effort in vain to construct a scaffold upon the 2-D surface.

It is clear that the presence of a third dimension is a prerequisite for a silkworm to encapsulate itself within a cocoon. Remarkably, the silkworm is able to survey its environment, evaluate the height available for anchor point placement, and react accordingly, presumably by comparing its own height against the height available in its surroundings for scaffold construction. Within a closed Petri dish, it is common for the silkworm to stand and prop the lid to create more upwards space

for itself, as shown in **Figure 19**. But in instances when it can not alter its spinning environment, it must decide how its silk will be spent. When a thin (7.5 mm tall) lid was used in these experiments, the silkworms invariably spun a mat, creating anchor points around the raised perimeter of the dish. However, use of a slightly taller (12.5 mm) dish led silkworms to successfully spin cocoons in which they could encapsulate themselves for safety. In a number of these instances, as seen in **Figure 20**, the cocoons assumed unusual, flatter, shapes where the aspect ratio was noticeably disproportionate relative to normal cocoons. Thus, it appears that a threshold height of approximately 1 cm exists below which mats are spun and above which cocoons are spun, something that the silkworm is able to determine through its primitive sets of eyes and sense of touch.

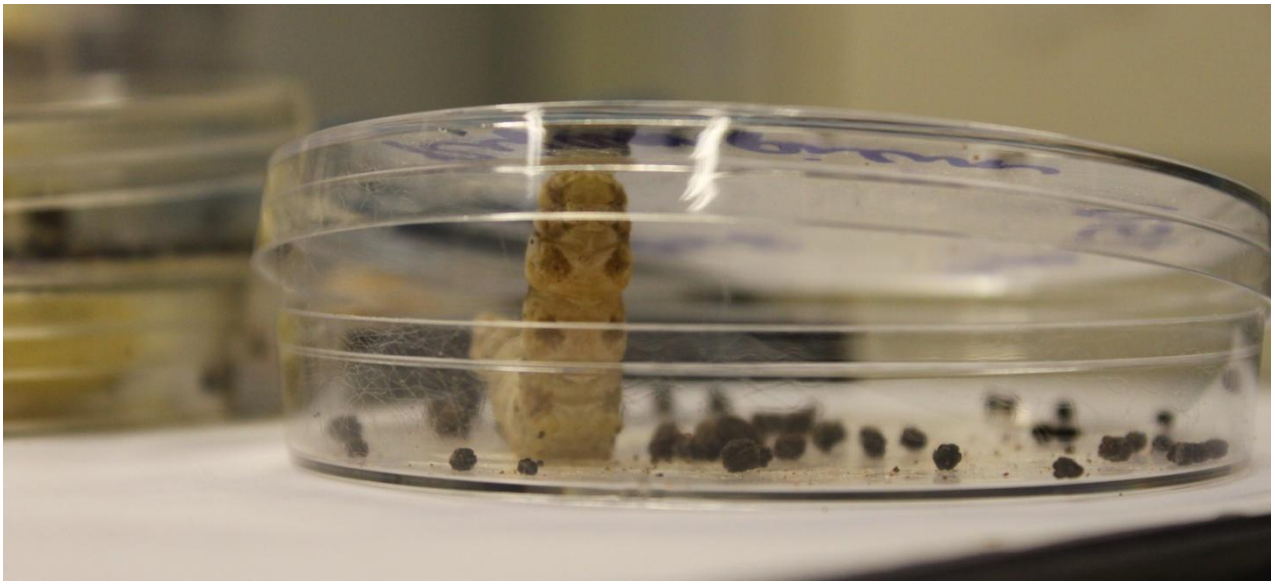

Figure 19. Silkworm propping petri dish lid in an effort to create sufficient height for cocoon spinning.

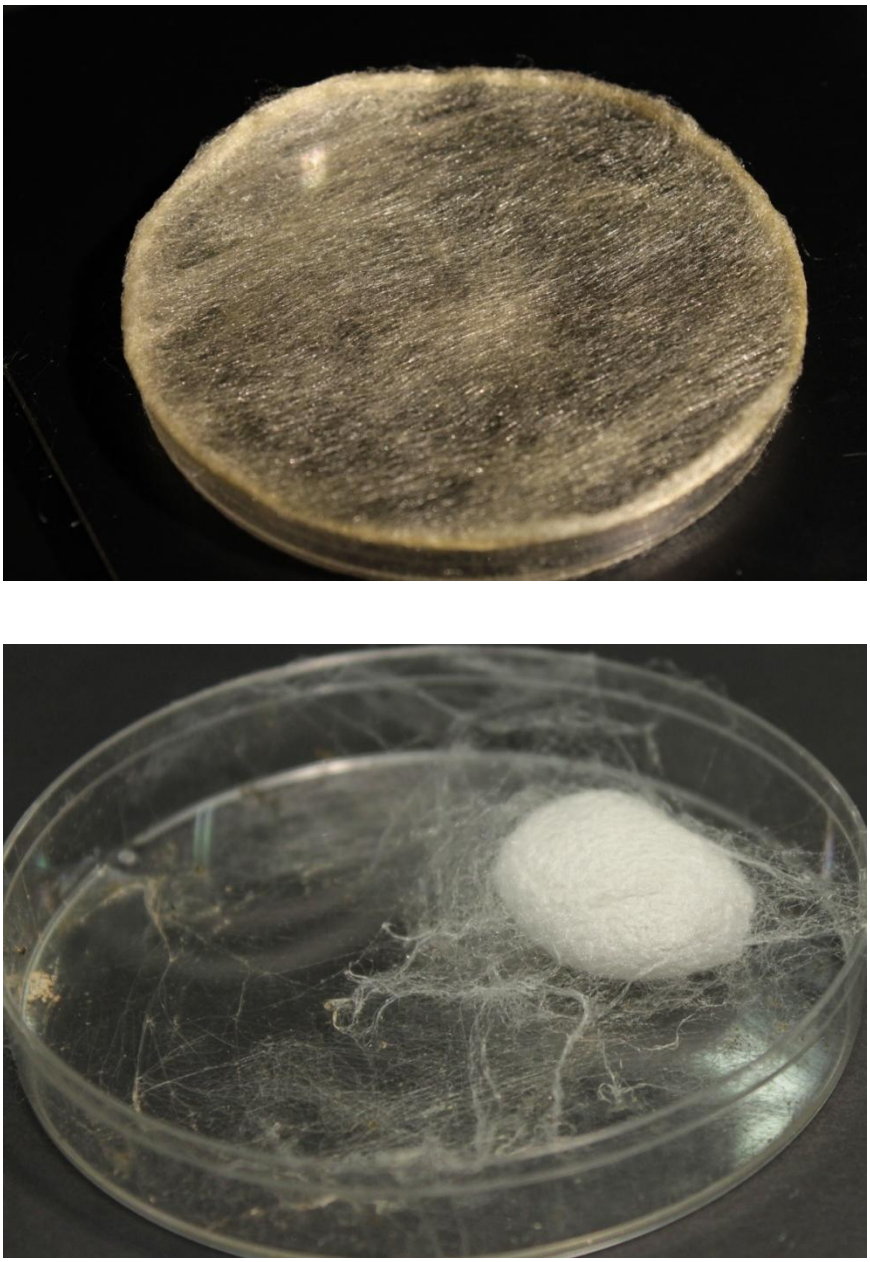

Figure 20. Silkworm spinning as a function of available height.
Top: a 7mm dish height results in a silk mat
Bottom: a 12 mm dish height results in a flattened cocoon

Efforts to obtain pyramid-shaped or prism-shaped cocoons were not successful. While the initial scaffold phase of spinning yielded fibers that fit the desired shapes, with a predilection for corners, as shown in **Figure 21**, the silkworms resumed more conventional spinning behavior once their anchor points were affixed, with an oval-shaped cocoon as the result, as shown in **Figure 22**.

Figure 21. Silkworm spinning atop a Teflon sheet, with one vertical anchor point available as well as the roughened edges of the cut Teflon sheet.

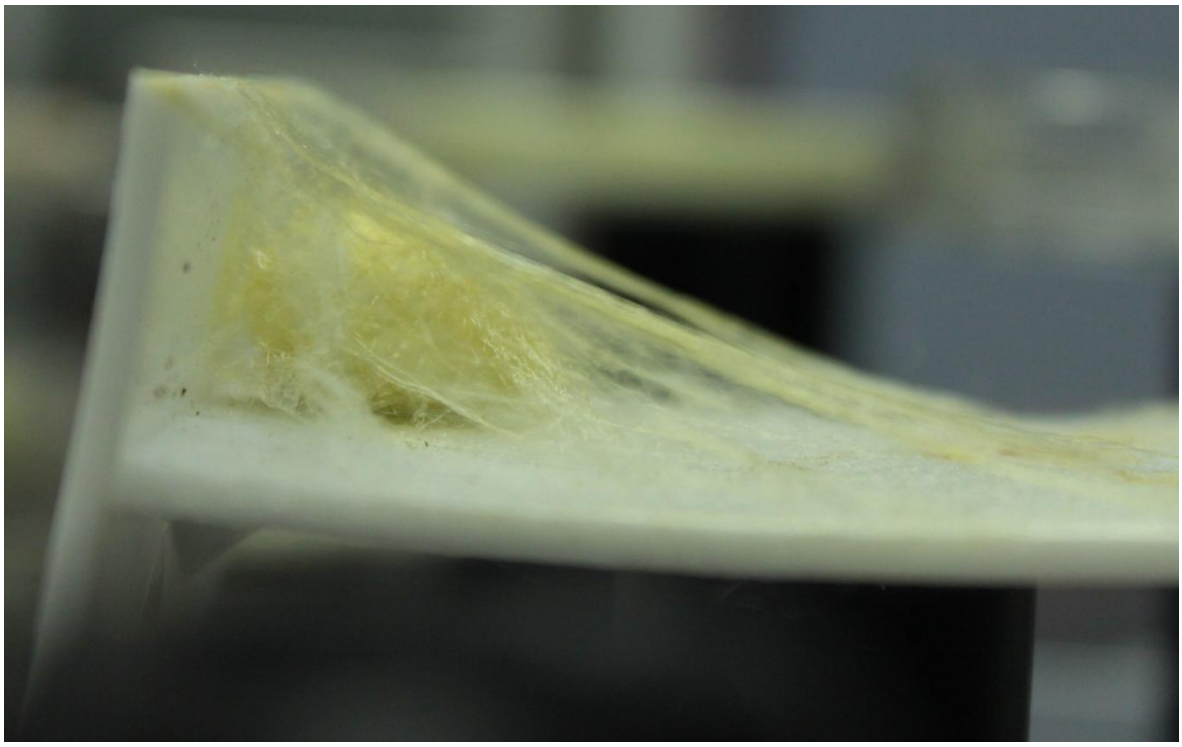

Figure 22. Silkworm scaffold atop Teflon conforms to available geometry, yet resulting cocoon is entirely regular.

iv. Discussion

A multitude of papers have examined the spinning behaviors of Bombyx mori silkworms, as well as other silk-producing creatures.[107-111] The roles of temperature, humidity, light exposure, and diet have been considered, as well as the value of different mounting materials and configurations, driven by the primary motivation of optimizing silk yield and quality for textile applications.[112] Studies of silkworm behavior have even extended to mathematical quantification of cocoon spinning patterns via methods including stochastic modeling and Fourier coefficients.[113-117] Yet observations about silk mats are rather limited. Van der Kloot, a graduate student at Harvard in the early 1950's, touched upon the idea briefly in an experiment where he had silkworms spinning inside inflated balloons.[106] Barton revisited the idea in an unsuccessful patent application less than a decade ago.[118] But this relatively simple idea remains largely unexplored.

The use of silk mats changes material processing requirements in a manner that can avail silk to a large number of people who otherwise would avoid it on the basis of religious and ethical objections, including Buddhists (405 million,) Hindus (920 million)[120] and Jains. The silkworm, when ready to emerge from a conventional cocoon, secretes cocoonases that discolor part of the cocoon and interrupt its continuous strand so that it can not be reeled easily.[121, 122] As a

preemptive measure, the standard process employs heat treatment to kill the pupa within its cocoon so that its silk is not compromised and can be harvested in its entirety. Without encapsulating the pupa, the process by which the mats are made is significant in that it does not kill the silkworm, in contrast to the conventional method of silk production.

In India, a process has been developed to reel the remaining silk after cocoons have been degraded by cocoonases, and this silk is known as 'ahimsa silk.[123] 'Ahimsa' is a Sanskrit word whose meaning, 'Do No Harm,' and reflects that the silkworm is not harmed in this silk's harvest. However, this alternate method of producing silk has a limited yield as a consequence of damage incurred by cocoonases. In contrast, though not yet proven, it is believed that mats formed by individual silkworms in the manner described in this chapter can be reeled in their entirely to match the silk harvest of a conventional cocoon, humanely.

Additionally, it is worthwhile to consider how intact mats might be used to make a usable product far more simply than alternate methods. As a cocoon, silk has interesting potential uses but limited utility. At present, it can be made useful only through reeling or solubilization, both of which require a number of additional processing steps. Silk mats may be able to occupy a niche within the textile trade through their ability to serve as fabrics that requiring no equipment beyond simple, flat spinning substrates.

6 CHEMICALLY-ENHANCED MATS

i. Introduction

The development of silk mats, while novel, may not be useful by itself. However, if chemical compounds could be integrated into the silk, these mats might prove useful as tools such as drug-eluting sheets or antibiotic fabrics. This effort expounds upon previous studies conducted by textile researchers, who fed dyes to silkworms and examined the response, hoping to produce colored cocoons.[124,125] Such studies date back to the mid 1800's and their pursuit has continued intermittently until the present day, most recently in a paper by Tansil published earlier this year.[126,127] Notably, none of the other studies aiming to modify the resultant silk investigated the prospect of feeding a molecule other than a dye, and the response to these molecules was quite varied.

The motivation behind this proof-of-principle study is to create silk cocoons and, by extension, mats containing other biologically-relevant molecules, including drugs. Such a result offers a markedly different approach to sustained release drug delivery, whereby the drug and its delivery system are produced together via a natural biological process, spinning. Moreover, these fibers may offer the ability to extend the viable lifespan of drugs, as shown previously with hemoglobin immobilized within silk films.[20]

What must be elucidated is the following: Which molecules, when fed to silkworm larvae through their food, will traverse the lining of the gut and incorporate preferentially within the silk gland, and why are they successful where others may not be? What sort of non-toxic dose, considering both concentration and number of feedings, is required to measure an acceptable level of the desired molecule within the spun silk? Finally, how does the distribution of the molecule between fibroin vs. sericin vary as a function of the drug?

ii. Methods: Chemical Compound Incorporation

For each unique molecular additive and concentration, the compound and reconstituted mulberry leaf food were carefully measured separately and then mixed together thoroughly. Color changes in many instances were pronounced.

Figure 23. Color changes within reconstituted mulberry leaf food with the addition of chemical compounds.

Table 3 lists the food additives that were employed in the first round experiments. The concentrations employed in this study were selected on the basis of previously published work. For each of the following drug samples, 5 silkworms were used, with the exception of litmus, for which 3 silkworms were used.

Molecule	***Mass /MW***	***Category***	***Concentration***		
Rhodamine B	479.02 amu	Dye	0.025%	0.05%	
Methylene Blue	319.85 amu	Dye	0.025%	0.05%	
Stilbene	180.25 amu	Dye	0.1%		
Rifampicin	822.94 amu	Antibiotic	0.025%	0.05%	0.5%
Gentamicin	477.60 amu	Antibiotic	0.5%		
Beta-carotene	536.87 amu	Antioxidant	0.025%	0.05%	
Horseradish Peroxidase (HRP)	44.17 kDa	Enzyme	0.025%	0.05%	
Gold Nanoparticles		Nanoparticles	0.5 mL (1x) in 22.6 g of food		
Litmus		pH sensor	0.08%		

Table 3. List of chemical compounds added to silkworm food in this experiment.

Rifampicin is a potent antibiotic typically used to treat Mycobacterium infections, including tuberculosis. It binds to DNA-dependent RNA polymerase, thereby inhibiting the initiation of RNA synthesis. Rifampicin is known to have low water solubility, and is readily absorbed from the human gastrointestinal tract. However, since resistance is common, if often is used in conjunction with other drugs in combination therapy.

Gentamicin is a aminoglycoside antibiotic, useful in treating many types of bacterial infection. It binds to a ribosomal subunit in the bacterium, thereby interrupting protein synthesis. Most notably, it is a heat-stable antibiotic that is capable of retaining activity even after autoclaving. Gentamicin is poorly absorbed across the digestive tract, and consequently is administered intravenously, intramuscularly or topically. Risks associated with this antibiotic include ototoxicity (particularly the vestibular organ) and nephrotoxicity.

In practice, the enzyme **horseradish peroxidase** (HRP), catalyzes the conversion of chromogenic substrates such as TMB (3,3’,5,5’-Tetramethylbenzidine), DAB (3,3'-Diaminobenzidine), or ABTS (2,2'-azino-bis(3-ethylbenzthiazoline-6-sulphonic acid)) into colored molecules.

Beta-carotene is a deeply colored red-orange pigment, abundant in plants and fruits, that is one of the primary dietary sources of pro-vitamin A. As a plant carotenoid, beta-carotene is absorbed into the human small intestine by passive diffusion. It is very lipophilic.

Methylene blue is a photosensitizer used to create singlet oxygen when exposed to both oxygen and light. As such, it is a useful drug applied in photodynamic therapy (PDT.) In addition, it is employed as a redox indicator that is colorless in a reducing environment but blue in an oxidizing one.

Rhodamine B (positive control) is a fluorescent dye with a peak excitation of 540 nm. It is a positive control in this experiment, replicating what was used in a recent paper by Tansil et al.[126]

Stilbene is used in the manufacture of dyes and optical brighteners. When excited by ultraviolet light, it emits blue visible light. It can be used as a gain medium in lasers. Moreover, stilbene derivatives, including resveratrol, are commonly found in plants.

Litmus is a water-soluble mixture of different dyes extracted from lichens, especially Roccella tinctoria. Used widely for pH sensing within solution, litmus turns red under acidic conditions and blue under basic ones.

Gold nanoparticles are prepared by adding 1% trisodium citrate to boiled 1.0 mM hydrogen tetrachloroaurate $HAuCl_4$ and heating briefly. The resulting solution is deep red in color and local increases in temperature can be measured when these nanoparticles are interrogated with green laser light.

Following spinning, the presence of the added compounds within the spun silk was validated using a host of tests as specified in the Results section.

iii. Results

A significant percentage of silkworms in this experiment demonstrated physical changes as a direct result of consuming the doped food. Larvae that consumed either rhodamine B or methylene blue yielded the most immediate and visibly obvious changes in the color of their integument, as shown in **Figure 24,** though it was not determined whether these changes manifest themselves within the cuticle, epidermis, or basement membrane.

Figure 24. Color changes in silkworms as a result of dye consumption. Silkworms fed rhodamine B turn distinctly red. Those fed methylene blue turn a more subtle shade of blue, visible upon comparison with the control silkworm shown in middle.

Moreover, these dyes also manifested themselves within the silk glands and the resulting cocoons. **Figure 25** depicts a cocoon spun by one silkworm that was fed rhodamine B. The cocoon is visibly pink in color on account of the dye. Additionally, rhodamine B dye, when excited with green light, emits in the yellow. Upon interrogation with green (532 nm) light from a laser pointer, the cocoon's fluorescence further validates the presence of rhodamine B within the silk.

With methylene blue, uptake within the silk glands appears far less pronounced than that in the reproductive organs. While the resulting silk cocoons showed a

very subtle blue color within predominantly yellow silk, the eggs laid by the adult moths were strongly blue in color, as shown in **Figure 26**, whereas normal eggs are distinctly yellow when laid.

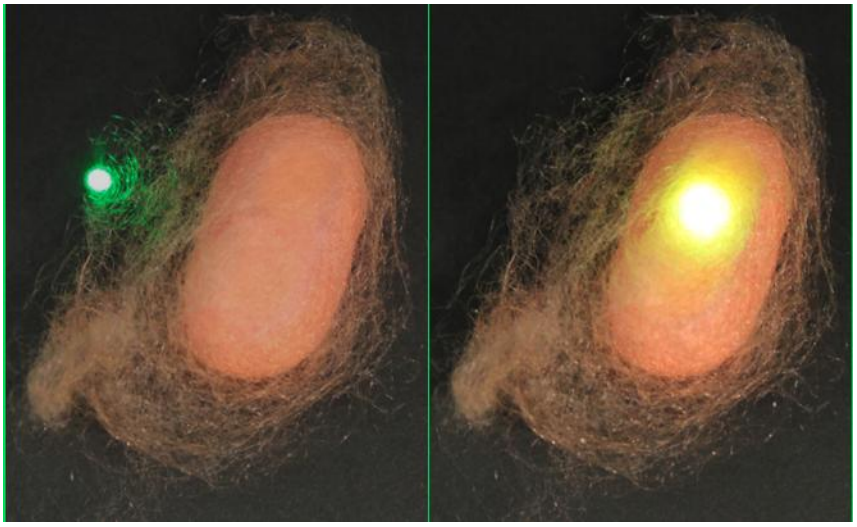

Figure 25. Fluorescence affirms the presence of rhodamine B within cocoons. Left: A 532 nm laser pointer was used as the excitation source. Right: Emission of light at a longer wavelength is apparent.

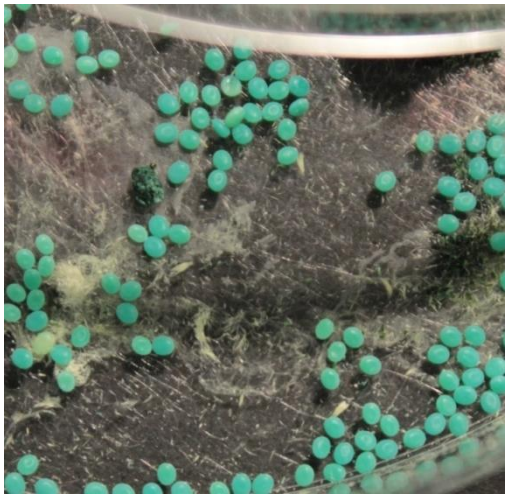

Figure 26. Eggs laid by adult moths fed methylene blue as silkworm larvae.

Uptake of active enzymes was studied through the use of HRP. Its presence in cocoon silk was evaluated through the use of a TMB (3,3',5,5'-Tetramethylbenzidine) test. TMB is a 240.35 g/mol molecule that, in solution, is initially colorless. It turns blue when allowed to react with peroxidase enzymes such as HRP. **Figure 27** positively confirms that functional HRP is carried from the food into the spun silk, turning blue, while ordinary silk remains colorless. Notably, the silk used in this experiment was derived from a silkworm who consumed less than two feedings' worth of HRP-containing food, suggesting that HRP is readily absorbed across the gut into the hemolymph. Though yet to be studied, this could be further reinforced by quantifying HRP content within the silkworm excrement.

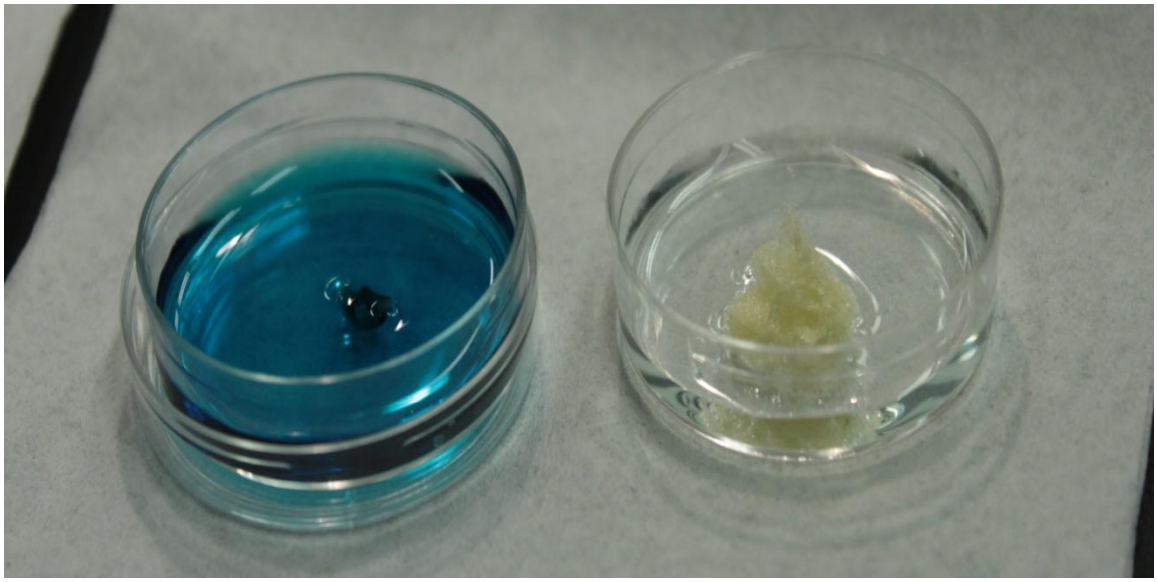

Figure 27. Confirmation that horseradish peroxidase enzyme incorporated into silkworm food manifests itself within silk spun by the larva. TMB test results from HRP silk (left) and normal silk (right).

Presence of the antibiotic rifampicin within silk was tested via placement of sample silk onto bacterial lawns comprised of *Stapylococcus aureus* bacteria. Lawns were cultured for 24 hours prior to the application of silk and then subsequently stored at 4°C for 24 hours prior to evaluation. As shown in **Figure 28**, a circular region of dead bacterial was evident around silk samples containing rifampicin, while no interruption was visible on the bacterial lawn where control silk was placed. This antibacterial effect was seen using all three concentrations of rifampicin that were employed, and grew more pronounced with increasing rifampicin dose. The presence of 0.5% gentamicin also was tested, and yet again antibiotic activity was evident, albeit less pronounced relative to a similar concentration of rifampicin.

An evaluation of survival rate offers some insight into the effectiveness of dose selections used in this study. **Table 4** shows silkworm response to this feeding as a function of molecular additive and concentration. Most notably, no adverse effects were observed across all concentrations of rifampicin. In contrast, half of the silkworms who were fed beta-carotene, more than half of those fed stilbene, all but one of the silkworms fed gold nanoparticles died.

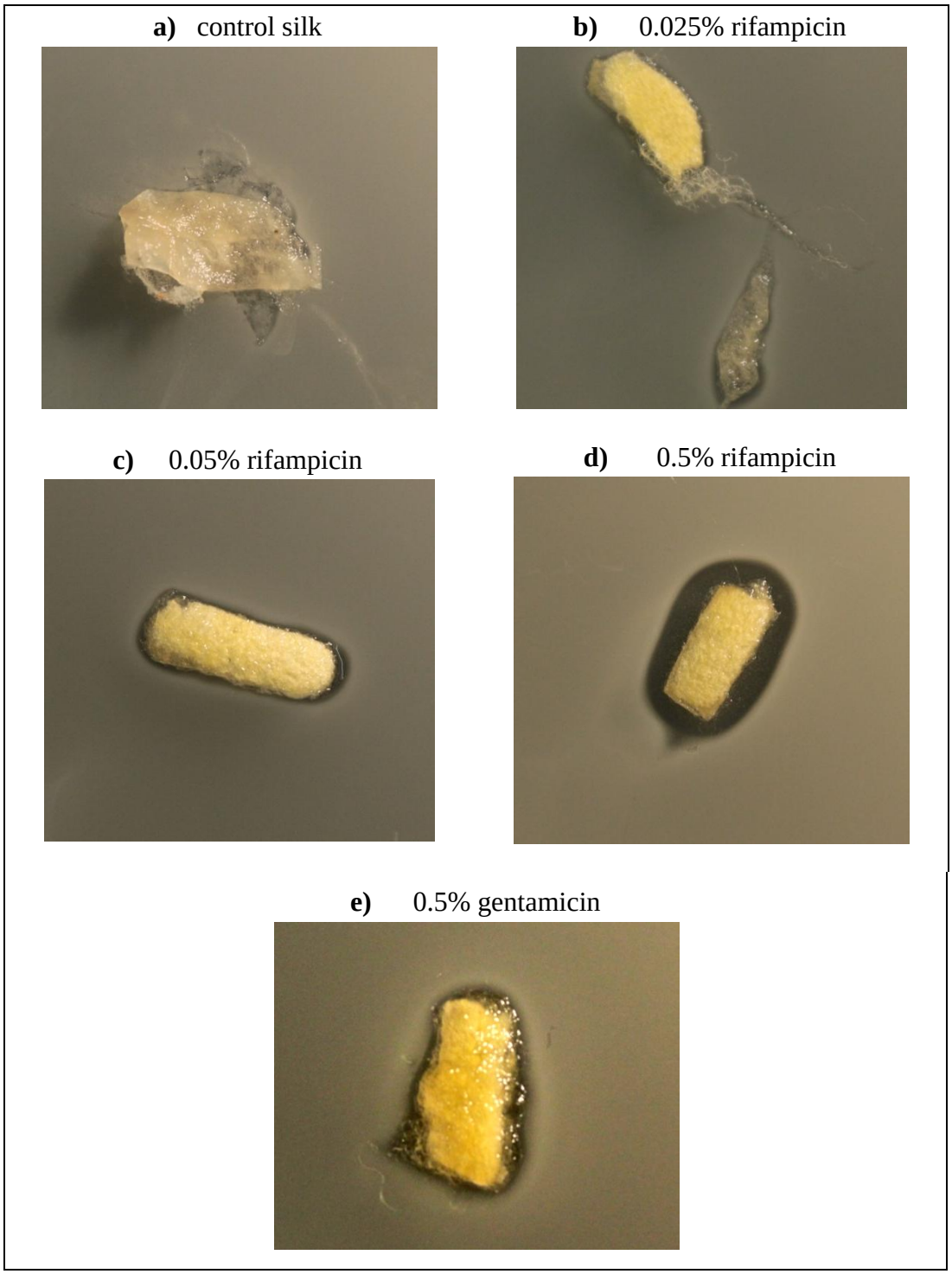

Figure 28. Evidence of the efficacy of antibiotic silk atop a bacterial lawn. Cocoons spun by 0.5% rifampicin-fed silkworms, resulted in a particularly pronounced halo effect signifying appreciable bacterial inhibition and death.

Molecule		**0-1 feedings**	**1-2 feedings**	**2-3 feedings**	**3-4 feedings**	**4+ feedings**	**Adverse effects**
Rhodamine B	0.025%	1	0	3	0	1	None
	0.05%	2	2	0	0	0	1 dead
Methylene Blue	0.025%	1	2	1	0	0	1 dead
	0.05%	2	1	1	1	0	None
Stilbene		0	0	0	1	1	3 dead
Rifampicin	0.025%	2	0	1	0	2	None
	0.05%	2	0	1	0	2	None
	0.5%	1	0	1	0	3	None
Gentamicin	0.5%	0	0	2	1	1	1 dead *
Beta-carotene	0.025%	0	0	0	0	3	2 dead
	0.05%	0	0	0	0	2	3 dead
Horseradish Peroxidase (HRP)	0.025%	2	1	2	0	0	None
	0.05%	1	2	0	1	1	1 dead *
Gold Nanoparticles		0	0	0	1	0	4 dead
Litmus **[3 worms]**		1	0	1	0	1	None

Table 4. Record of when silkworms commenced spinning, as a function of number of meals consumed with the addition of chemical compounds, and resulting outcomes. Asterisks represent intraspinning deaths.

Towards addressing the distribution of antibiotics between fibroin and sericin, cocoon fragments from silkworms fed a 0.5% rifampicin or 0.5% gentamicin diet were boiled in 5 milliliters of milli-Q water for 1 minute with gentle stirring. The cocoon segments were then bathed in milli-Q water at room temperature to remove residual sericin. The sericin released during boiling was collected by absorption with filter paper. Each piece of degummed silk and each piece of filter paper containing liquid sericin was deposited onto a separate bacterial lawn and re-evaluated after 24 hours. No differences were observed between the control lawn and sericin samples from either the rifampicin or the gentamicin silk. Fibroin from the degummed gentamicin sample showed a comparable lack of bioactivity. Fibroin from the degummed rifampicin sample, however, retained some bioactivity, as shown in **Figure 29**. This result validates that rifampicin content is prominent within the silk fibers themselves, as bioactivity was discernable even in the sample's compromised, post-boiling state.

Figure 29. Silk containing rifampicin placed atop a bacterial lawn after degumming for 1 minute in boiling milli-Q water. The silk retains some of its antibiotic property. Loss of bioactivity is attributed to high temperature degradation.

iv. Discussion

The results presented here demonstrate conclusively that the silkworm is capable of absorbing select drugs and enzymes across its gut and into the silk glands where these molecules are incorporated into the silk that is spun. Thus, an additional method has been introduced using silk as a potential vehicle for drug delivery.[128,129] Indeed, many questions remain in explaining why some molecules navigate successfully to the silk glands while others do not. Silkworm physiology presents a number of sequential steps where problems may arise. First is acceptance of the food; the silkworm uses its receptors for smell and taste to decide what to eat. The addition of some molecules to its food, namely gold nanoparticles and stilbene, led the silkworms to eat very sparingly, or not at all. In contrast, silkworms who received gentamicin or litmus ate heartily and grew quickly. One must consider how this process might be influenced to add to the set of viable molecules through encapsulation, co-loading, or some alternate chemical modification. Of course, dosimetry will also play a role here; much remains to be studied towards elucidating the unique nontoxic concentration range for each administered molecule. For some seemingly unpalatable ones, a less concentrated dose may prove amenable for silkworm acceptance and hopefully remain sufficient for an acceptable level to be measured within the spun silk.

Second, interactions within the digestive tract must be evaluated further. The silkworm attempts to change insoluble substances within its food into soluble ones, through digestion via saliva and gastric juice prior to absorption across the lining of the midgut and hindgut. **Table 5** offers a list of enzymes to which food is exposed while passing through the digestive tract. These interactions may prove deleterious to some molecules by compromising their bioactivity.

Gastric juice components	**Role**
Tyrosinase	*A protease with oxidizing properties*
Lipase	*A fat-decomposing enzyme*
Amylase	*Decomposes starch into dextrin and maltase*
Maltase & Glycogenase	*Carbohydrate-decomposing enzymes*
Oxidase, Peroxidase & Catalase	*Oxidizing enzymes*
In cells of intestine	**Role**
Invertase	*Decomposes sucrose into glucose and fructose*
Galactase	*Hydrolyzes galactan into glucose and fructose (or galactose)*

Table 5. List of enzymes to which chemical compounds are exposed through oral delivery.[28]

Next, substances that are successfully absorbed across the intestine are introduced into the hemolymph, which can carry them throughout the body via the silkworm open circulatory system. Some molecules, such as HRP and rifampicin, migrate adequately to the silk glands at the concentrations used in this work. Others molecules, such as methylene blue, do not, preferentially migrating elsewhere, such as to the reproductive organs. Towards understanding which molecules are most innately well-suited for targeted delivery to the silk glands, the partition coefficient, P, is a useful variable. Used in pharmaceutical science as well as organic chemistry, it measures how well a substance partitions between an organic solvent and water. Log P values are regarded as a measure of lipophilicity, and each organ is seen as possessing its own unique spectrum of log P values allowing for optimal absorption. What remains to be determined is the set of ideal ranges corresponding to silkworm organs.

On a finer scale, for molecules that are successfully integrated into silk fiber, the distribution between fibroin and sericin must be examined. This is particularly significant when considering that most applications require the removal of sericin via degumming as a necessary step. Tansil considered this matter and, with a small set of dyes, showed that maximum fibroin uptake is realized when log P > 2.2. Physiologically, this corresponds to optimal absorption in the posterior and middle portions of the gland. Alternatively, a log P value of 0.6, reflecting

maximum uptake in sericin, likely corresponds to optimal absorption in the anterior part of the silk gland, where sericin is at its most prevalent.

Bioactivity from degummed silk containing either rifampicin or gentamicin agrees with Tansil's fibroin prediction, considering experimentally calculated log P values for rifampicin (2.7) and gentamicin (-3.1).[130,131] With a log P value greater than 2.2, it is believed that silk fibroin retains a sufficient mass of rifampicin, thereby maintaining bioactivity. In contrast, with a negative log P value, gentamicin is believed to reside primarily within sericin; thus after degumming, the remaining fibroin is unable to produce any noticeable effect upon a bacterial lawn.

While chemically-enhanced mats were the initial aim in this work, another prospective application may be found in the use of drug-loaded sutures, realized by feeding these chemical compounds to cocoons, or alternatively injecting these chemicals into the glands directly or the surrounding hemolymph, and then reeling the conventionally-shaped cocoons that they spin. A movement towards drug-loaded sutures has already emerged, with materials including silk.[132] However, these other efforts have only attempted to coat the outer fiber surface.[133,134, 135] The promise offered by the prospective silk sutures presented here is that drug may be released throughout the entire timeframe of suture

degradation. Unfortunately however, that duration, or release profile, can not be easily programmed in a manner comparable to what can be realized with the annealing of materials produced from regenerated silk solution.[136]

The matter of dose similarity is another issue that must be considered. While each silkworm consumes a different volume of food and spins a cocoon of unique mass, it remains unclear how much variability exists in terms of drug mass per unit length of fiber, for a fixed concentration of drug within the mulberry diet. One study examining variations in spinning efficiency across genotypes measured the food that was consumed and the mass of the resulting cocoon shell. The author showed a factor of two difference in efficiency between the two most extreme cases, but variability within a single genotype, likely to be far less, was not examined.[137]

For most applications, sericin removal is warranted. The means of degumming merit further study. The most conventional approach to degumming, boiling at 100°C in a $NaCO_3$ solution, poses an inherent limitation: it compromises the bioactivity of many molecules. It is known, for example, that HRP loses bioactivity at temperatures greater than 60°C. Similarly, rifampicin loses bioactivity at temperatures above 40°C. This discord highlights the need for a low-temperature degumming method that may preserve optimal bioactivity for temperature-sensitive molecules.[70,138,139]

7 CONCLUSION

While silk possesses an extensive history, it is enjoying a newfound allure spurred by emerging opportunities in sensing, tissue engineering and drug delivery. What is presented here represents two new approaches to the manipulation of silk, introducing novel techniques that expound upon silk's demonstrated capabilities. E-gel films are unique in that they allow for unconventional topologies to be formed, offering the prospect of conformal silk layers with extended degradation times and greater thicknesses relative to previously published work.[65] These advantages lend to applications that include targeted drug delivery and stratified engineered tissues. As well, the low surface roughness and ease of fabrication are of interest in the realm of optics. Natural silk mats, when supplemented with chemical compounds, also allow for the slow, prolonged release of drugs; further, the approach presented here offers promise for applications that include advanced sutures and the creation of antibacterial fabrics.

Still, important challenges remain to be addressed should either of these technologies be scaled. With e-gel films, a glaring need exists for a method capable of producing large volumes of silk solution possessing both intra- and inter-batch consistency. Towards generating e-gel films reproducibly, one must consider that the e-gel response to electrical stimulation is a function of silk solution conditions, making this level of control a critical requirement in scaling and automation. Some have proposed the use of genetically engineered silk as an

alternative; the advantages of this type of silk are that it can be made in relatively larger volumes, that it circumvents the harsh degumming step entirely, and that it eliminates the intra- and inter-cocoon variability in protein amino acid composition.[140,141] However, molecular weight constraints make the full heavy chain difficult to replicate transgenetically, and it remains to be seen how such a solution might respond to an applied current. For any viable solution, natural or transgenic, concerns are high regarding changes in protein conformation over time, as they are difficult to regulate predictably and present progressive increases in silk β-sheet content. In total, these challenges for silk solution truly are far from trivial.

With natural silk mats containing select drugs or other chemical additives, a particular need remains for a gentle degumming technique. It is believed that the presence of sericin elicits an immune response within the body and therefore must be removed appreciably.[142] The current standard for degumming, however, must be reconciled: boiling in sodium carbonate solution, a technique dating back to at least 1762[143], leverages the fact that sericins are far more water-soluble than fibroin, and that sericins are susceptible to alkalinity; yet, this approach comes with a cost: compromising the bioactivity of a significant fraction of prospective drugs.

Use of a low-pressure plasma treatment, recently explored as an adjunct to conventional degumming, represents one prospective alternative to high-temperature alkaline solutions, having been shown to produce an etching effect on the fiber surface.[144] Oxygen plasma, a more desirable choice for biomedical use, has not yet been studied in the context of degumming, but has been shown to produce a similar etching effect in already-degummed silk fibers.[145,146,147] What is significant about the use of plasma, beyond degumming, is that it also is effective for sterilization, overcoming the limitations that heat-, chemical-, and UV light-based techniques pose in the sterilization of implantable silk devices.[148, 149,150] Further, plasma treatment has been shown to be a cost-effective technique by comparison with conventional methods including steam sterilization and ethylene oxide (cold gas) treatment.[151]

---

[1] United Nations Food and Agriculture Organization *in Conservation Status of Sericulture Germplasm Resources in the World* 168 (New York, NY 2003).

[2] 21CFR878.5030

[3] Perez-Rigueiro, J., Viney, C., Llorca, J. & Elices, M. Silkworm silk as an engineering material. *J Appl Polym Sci* **70**, 2439-2447 (1998).

[4] Altman, G. H. *et al*. Silk-based biomaterials. *Biomaterials* **24**, 401-416 (2003).

[5] Hardy, J. G., Romer, L. M. & Scheibel, T. R. Polymeric materials based on silk proteins. *Polymer* **49**, 4309-4327 (2008).

[6] Hardy, J. G. & Scheibel, T. R. Silk-inspired polymers and proteins. *Biochem. Soc. Trans.* **37**, 677-681 (2009).

[7] Omenetto, F. G. & Kaplan, D. L. A new route for silk. *Nature Photonics* **2**, 641-643 (2008).

[8] Omenetto, F. G. & Kaplan, D. L. New Opportunities for an Ancient Material. *Science* **329**, 528-531 (2010).

[9] Omenetto, F. & Kaplan, D. From Silk Cocoon to Medical Miracle. *Sci. Am.* **303**, 76-77 (2010).

[10] Vepari, C. & Kaplan, D. L. Silk as a biomaterial. *Progress in Polymer Science* **32**, 991-1007 (2007).

[11] Parker, S. T. *et al*. Biocompatible Silk Printed Optical Waveguides. *Adv Mater* **21**, 2411-2415 (2009).

[12] Omenetto, F. G. & Kaplan, D. L. SnapShot: Silk biomaterials. *Biomaterials* **31**, 6119-20 (2010).

[13] Nazarov, R., Jin, H. J. & Kaplan, D. L. Porous 3-D scaffolds from regenerated silk fibroin. *Biomacromolecules* **5**, 718-726 (2004).

[14] He, S. J., Valluzzi, R. & Gido, S. P. Silk I structure in Bombyx mori silk foams. *Int. J. Biol. Macromol.* **24**, 187-195 (1999).

[15] Cao, Z. B., Chen, X., Yao, J. R., Huang, L. & Shao, Z. Z. The preparation of regenerated silk fibroin microspheres. *Soft Matter* **3**, 910-915 (2007).

[16] Zhang, Y. Q. *et al*. Formation of silk fibroin nanoparticles in water-miscible organic solvent and their characterization. *Journal of Nanoparticle Research* **9**, 885-900 (2007).

[17] Lawrence, B. D., Cronin-Golomb, M., Georgakoudi, I., Kaplan, D. L. & Omenetto, F. G. Bioactive silk protein biomaterial systems for optical devices. *Biomacromolecules* **9**, 1214-1220 (2008).

[18] Perry, H., Gopinath, A., Kaplan, D. L., Dal Negro, L. & Omenetto, F. G. Nano- and micropatterning of optically transparent, mechanically robust, biocompatible silk fibroin films. *Adv Mater* **20**, 3070-3072 (2008).

[19] Amsden, J. J. *et al*. Rapid Nanoimprinting of Silk Fibroin Films for Biophotonic Applications. *Adv Mater* **22**, 1746-1749 (2010).

[20] Domachuk, P., Perry, H., Amsden, J. J., Kaplan, D. L. & Omenetto, F. G. Bioactive "self-sensing" optical systems. *Appl. Phys. Lett.* **95** (2009).

[21] Tao, H. *et al*. Metamaterial Silk Composites at Terahertz Frequencies. *Adv Mater* **22**, 3527-3531 (2010).

[22] Leisk, G. G., Lo, T. J., Yucel, T., Lu, Q. & Kaplan, D. L. Electrogelation for Protein Adhesives. *Adv Mater* **22**, 711-715 (2010).

[23] Matthews, J. M. in *The Textile Fibres. Their Physical, Microscopical, and Chemical Properties* 323 (J. Wiley & Sons, New York, N.Y., 1904).

[24] Chen, F., Porter, D. & Vollrath, F. Silkworm cocoons inspire models for random fiber and particulate composites. *Physical Review E* **82** (2010).

[25] Hruska, J. F., Felsted, R. L. & Law, J. H. Cocoonases of Silkworm Moths - Catalytic Properties and Biological Function. *Insect Biochemistry* **3**, 31-43 (1973).

[26] Falakali, B. & Turgay, G. Some morphological features of the rectal sac of the silkworm (Bombyx mori: Bombycidae). *Turkish Journal of Zoology* **23**, 427-432 (1999).

[27] Banno, Y., Shimada, T., Kajiura, Z. & Sezutsu, H. The Silkworm-An Attractive BioResource Supplied by Japan. *Experimental Animals* **59**, 139-146 (2010).

[28] Shamsuddin, M. in *Silkworm Physiology: A Concise Textbook* 212 (Daya, New Delhi, India, 2009).

[29] Akai, H. The Structure and Ultrastructure of the Silk Gland. *Experientia* **39**, 443-449 (1983).

[30] Lydon,J. E. Silk: the original liquid crystalline polymer *Liquid Crystals Today* **13:3**, 1-13 (2004).

[31] Perez-Rigueiro, J., Elices, M., Llorca, J. & Viney, C. Tensile properties of silkworm silk obtained by forced silking. *J Appl Polym Sci* **82**, 1928-1935 (2001).

[32] Li, G. Y. *et al*. The natural silk spinning process - A nucleation-dependent aggregation mechanism? *European Journal of Biochemistry* **268**, 6600-6606 (2001).

[33] Magoshi, J. *et al*. Crystallization of silk fibroin from solution. *Thermochimica Acta* **352**, 165-169 (2000).

[34] Zhu, J. X., Zhang, Y. P., Shao, H. L. & Hu, X. C. Electrospinning and rheology of regenerated Bombyx mori silk fibroin aqueous solutions: The effects of pH and concentration. *Polymer* **49**, 2880-2885 (2008).

[35] Yamaura, K., Okumura, Y., Ozaki, A. & Matsuzawa, S. Flow-Induced Crystallization of Bombyx-Mori L Silk Fibroin from Regenerated Aqueous-Solution and Spinnability of its Solution. *Applied Polymer Symposia*, 205-220 (1985).

[36] Scheibel, T. Silk - a biomaterial with several facets. *Applied Physics A-Materials Science & Processing* **82**, 191-192 (2006).

[37] Kerkam, K., Viney, C., Kaplan, D. & Lombardi, S. Liquid Crystallinity of Natural Silk Secretions. *Nature* **349**, 596-598 (1991).

[38] Foo, C. W. P. *et al*. Role of pH and charge on silk protein assembly in insects and spiders. *Applied Physics A-Materials Science & Processing* **82**, 223-233 (2006).

[39] Terry, A. E., Knight, D. P., Porter, D. & Vollrath, F. PH induced changes in the rheology of silk fibroin solution from the middle division of Bombyx mori silkworm. *Biomacromolecules* **5**, 768-772 (2004).

[40] Zhou, P. *et al*. Effects of pH and calcium ions on the conformational transitions in silk fibroin using 2D Raman correlation spectroscopy and C-13 solid-state NMR. *Biochemistry (N. Y.)* **43**, 11302-11311 (2004).

[41] Asakura, T. *et al*. Some observations on the structure and function of the spinning apparatus in the silkworm Bombyx mori. *Biomacromolecules* **8**, 175-181 (2007).

[42] Moriya, M., Ohgo, K., Masubuchi, Y. & Asakura, T. Flow analysis of aqueous solution of silk fibroin in the spinneret of Bombyx mori silkworm by combination of viscosity measurement and finite element method calculation. *Polymer* **49**, 952-956 (2008).

[43] Breslauer, D. N., Lee, L. P. & Muller, S. J. Simulation of Flow in the Silk Gland. *Biomacromolecules* **10**, 49-57 (2009).

[44] Rossle, M., Panine, P., Urban, V. S. & Riekel, C. Structural evolution of regenerated silk fibroin under shear: Combined wide- and small-angle x-ray scattering experiments using synchrotron radiation. *Biopolymers* **74**, 316-327 (2004).

[45] Yamaura, K., Okumura, Y. & Matsuzawa, S. Mechanical Denaturation of High Polymers in Solutions .36. Flow-Induced Crystallization of Bombyx-Mori L Silk Fibroin from the Aqueous-Solution Under a Steady-State Flow. *Journal of Macromolecular Science-Physics* **B21**, 49-69 (1982).

[46] Xie, F., Zhang, H. H., Shao, H. L. & Hu, X. C. Effect of shearing on formation of silk fibers from regenerated Bombyx mori silk fibroin aqueous solution. *Int. J. Biol. Macromol.* **38**, 284-288 (2006).

[47] Iizuka, E. Mechanism of fiber formation by the silkworm, Bombyx mori L. *Biorheology* **3**, 141-152 (1966).

[48] Iizuka, E. The Physicochemical Properties of Silk Fibers and the Fiber Spinning Process. *Experientia* **39**, 449-454 (1983).

[49] Iizuka, E. Silk Thread - Mechanism of Spinning and its Mechanical-Properties. *Applied Polymer Symposia*, 173-185 (1985).

[50] Jin, H. J. & Kaplan, D. L. Mechanism of silk processing in insects and spiders. *Nature* **424**, 1057-1061 (2003).

[51] Wang, X. Y., Kim, H. J., Xu, P., Matsumoto, A. & Kaplan, D. L. Biomaterial coatings by stepwise deposition of silk fibroin. *Langmuir* **21**, 11335-11341 (2005).

[52] Zhou, L. *et al*. Copper in the silk formation process of Bombyx mori silkworm. *FEBS Lett.* **554**, 337-341 (2003).

[53] Nakagaki, I. & Sasaki, S. Secretory Potential and Ionic Transport in the Posterior Silk Glands of Bombyx-Mori. *J. Exp. Biol.* **134**, 155-171 (1988).

[54] Ruan, Q. X. & Zhou, P. Sodium ion effect on silk fibroin conformation characterized by solid-state NMR and generalized 2D NMR-NMR correlation. *J. Mol. Struct.* **883**, 85-90 (2008).

[55] Zhou, L., Chen, X., Shao, Z. Z., Huang, Y. F. & Knight, D. P. Effect of metallic ions on silk formation the mulberry silkworm, Bombyx mori. *J Phys Chem B* **109**, 16937-16945 (2005).

[56] Ruan, Q. X., Zhou, P., Hu, B. W. & Ji, D. An investigation into the effect of potassium ions on the folding of silk fibroin studied by generalized two-dimensional NMR-NMR correlation and Raman spectroscopy. *Febs Journal* **275**, 219-232 (2008).

[57] Ha, S. W., Tonelli, A. E. & Hudson, S. M. Structural studies of Bombyx mori silk fibroin during regeneration from solutions and wet fiber spinning. *Biomacromolecules* **6**, 1722-1731 (2005).

[58] Zhou, G. Q., Shao, Z. Z., Knight, D. P., Yan, J. P. & Chen, X. Silk Fibers Extruded Artificially from Aqueous Solutions of Regenerated Bombyx mori Silk Fibroin are Tougher than their Natural Counterparts. *Adv Mater* **21**, 366-370 (2009).

[59] Perez-Rigueiro, J. *et al*. Supramolecular organization of regenerated silkworm silk fibers. *Int. J. Biol. Macromol.* **44**, 195-202 (2009).

[60] Liivak, O., Blye, A., Shah, N. & Jelinski, L. W. A microfabricated wet-spinning apparatus to spin fibers of silk proteins. Structure-property correlations. *Macromolecules* **31**, 2947-2951 (1998).

[61] Matsumoto, K., Uejima, H., Iwasaki, T., Sano, Y. & Sumino, H. Studies on regenerated protein fibers .3. Production of regenerated silk fibroin fiber by the self-dialyzing wet spinning method. *J Appl Polym Sci* **60**, 503-511 (1996).

[62] Marsano, E. *et al*. Wet spinning of Bombyx mori silk fibroin dissolved in N-methyl morpholine N-oxide and properties of regenerated fibres. *Int. J. Biol. Macromol.* **37**, 179-188 (2005).

[63] Um, I. C. *et al*. Wet spinning of silk polymer - I. Effect of coagulation conditions on the morphological feature of filament. *Int. J. Biol. Macromol.* **34**, 89-105 (2004).

[64] Um, I. C. *et al*. Wet spinning of silk polymer - II. Effect of drawing on the structural characteristics and properties of filament. *Int. J. Biol. Macromol.* **34**, 107-119 (2004).

[65] Zhao, C. H., Yao, J. M., Masuda, H., Kishore, R. & Asakura, T. Structural characterization and artificial fiber formation of Bombyx mori silk fibroin in hexafluoro-iso-propanol solvent system. *Biopolymers* **69**, 253-259 (2003).

[66] Kim, D. H. *et al*. Dissolvable films of silk fibroin for ultrathin conformal bio-integrated electronics. *Nature Materials* **9**, 511-517 (2010).

[67] Amiraliyan, N., Nouri, M. & Kish, M. H. Effects of Some Electrospinning Parameters on Morphology of Natural Silk-Based Nanofibers. *J Appl Polym Sci* **113**, 226-234 (2009).

[68] Amiraliyan, N., Nouri, M. & Kish, M. H. Electrospinning of silk nanofibers. I. An investigation of nanofiber morphology and process optimization using response surface methodology. *Fibers and Polymers* **10**, 167-176 (2009).

[69] Coleman, D. & Howitt, F. O. Studies on Silk Proteins .1. the Properties and Constitution of Fibroin - the Conversion of Fibroin into a Water-Soluble Form and its Bearing on the Phenomenon of Denaturation. *Proceedings of the Royal Society of London Series A-Mathematical and Physical Sciences* **190**, 145-169 (1947).

[70] Yamada, H., Nakao, H., Takasu, Y. & Tsubouchi, K. Preparation of undegraded native molecular fibroin solution from silkworm cocoons. *Materials Science & Engineering C-Biomimetic and Supramolecular Systems* **14**, 41-46 (2001).

[71] Sah, M. & Pramanik, K. Regenerated Silk Fibroin from B. mori Silk Cocoon for Tissue Engineering Applications. *Proceedings of 2010 International Conference on Biotechnology and Food Science (Icbfs 2010)*, 206-212 (2010).

[72] Rajkhowa, R., Wang, L. J., Kanwar, J. R. & Wang, X. G. Molecular Weight and Secondary Structure Change in Eri Silk During Alkali Degumming and Powdering. *J Appl Polym Sci* **119**, 1339-1347 (2011).

[73] Zuo, B., Dai, L. & Wu, Z. Analysis of structure and properties of biodegradable regenerated silk fibroin fibers. *J. Mater. Sci.* **41**, 3357-3361 (2006).

[74] Sashina, E. S., Bochek, A. M., Novoselov, N. P. & Kirichenko, D. A. Structure and solubility of natural silk fibroin. *Russian Journal of Applied Chemistry* **79**, 869-876 (2006).

[75] Sagar, A. J., Rao, M. S. N. & Pandit, M. W. Properties of Silk Proteins Extracted in Saturated Lithium Thiocyanate Solution. *Indian J. Biochem. Biophys.* **15**, 59-61 (1978).

[76] Holland, C., Terry, A. E., Porter, D. & Vollrath, F. Natural and unnatural silks. *Polymer* **48**, 3388-3392 (2007).

[77] Zheng, S. D., Li, G. X., Yao, W. H. & Yu, T. Y. Raman-Spectroscopic Investigation of the Denaturation Process of Silk Fibroin. *Appl. Spectrosc.* **43**, 1269-1272 (1989).

[78] Yucel, T., Kojic, N., Leisk, G. G., Lo, T. J. & Kaplan, D. L. Non-equilibrium silk fibroin adhesives. *J. Struct. Biol.* **170**, 406-412 (2010).

[79] Maniglio, D. *et al*. Electrodeposition of Silk Fibroin on Metal Substrates. *J. Bioact. Compatible Polym.* **25**, 441-454 (2010).

[80] Boccaccini, A. R., Keim, S., Ma, R., Li, Y. & Zhitomirsky, I. Electrophoretic deposition of biomaterials. *Journal of the Royal Society Interface* **7**, S581-S613 (2010).

[81] Liu, Y. *et al*. Biofabrication to build the biology-device interface. *Biofabrication* **2** (2010).

[82] Shi, X. W. *et al*. Chitosan biotinylation and electrodeposition for selective protein assembly. *Macromolecular Bioscience* **8**, 451-457 (2008).

[83] Shi, X. W. *et al*. Reagentless Protein Assembly Triggered by Localized Electrical Signals. *Adv Mater* **21**, 984-988 (2009).

[84] Ma, R., Epand, R. F. & Zhitomirsky, I. Electrodeposition of hyaluronic acid and hyaluronic acid-bovine serum albumin films from aqueous solutions. *Colloids and Surfaces B-Biointerfaces* **77**, 279-285 (2010).

[85] Yi, H. M. *et al*. Biofabrication with chitosan. *Biomacromolecules* **6**, 2881-2894 (2005).

[86] Cheong, M. & Zhitomirsky, I. Electrodeposition of alginic acid and composite films. *Colloids and Surfaces A-Physicochemical and Engineering Aspects* **328**, 73-78 (2008).

[87] Kim, U. J. *et al*. Structure and properties of silk hydrogels. *Biomacromolecules* **5**, 786-792 (2004).

[88] Dicko, C., Kenney, J. M., Knight, D. & Vollrath, F. Transition to a beta-sheet-rich structure in spidroin in vitro: The effects of pH and cations. *Biochemistry (N. Y.)* **43**, 14080-14087 (2004).

[89] Li, X. G. et al. Conformational transition and liquid crystalline state of regenerated silk fibroin in water.*Biopolymers* **89**, 497-505 (2008).

[90] Ayub, Z. H., Arai, M. & Hirabayashi, K. Mechanism of the Gelation of Fibroin Solution. *Bioscience Biotechnology and Biochemistry* **57**, 1910-1912 (1993).

[91] Asakura, T., Sugino, R., Yao, J. M., Takashima, H. & Kishore, R. Comparative structure analysis of tyrosine and valine residues in unprocessed silk fibroin (silk I) and in the processed silk fiber (silk II) from Bombyx mori using solid-state C-13, N-15, and H-2 NMR. *Biochemistry (N. Y.)* **41**, 4415-4424 (2002).

[92] Yang, Y. H., Shao, Z. Z. & Chen, X. Influence of pH value on the structure of regenerated Bombyx mori silk fibroin in aqueous solution by optical spectroscopy. *Acta Chimica Sinica* **64**, 1730-1736 (2006).

[93] Sookine, A. M. & Harris, M. Electrophoretic Studies of Silk. *Textile Research* **9**, 374-383 (1939).

[94] Nagarkar, S., Nicolai, T., Chassenieux, C. & Lele, A. Structure and gelation mechanism of silk hydrogels. *Physical Chemistry Chemical Physics* **12**, 3834-3844 (2010).

[95] Popescu, R. *et al*. Biopolymer Thin Films for Optoelectronics Applications. *Molecular Crystals and Liquid Crystals* **522**, 529-537 (2010).

[96] Popescu, R., Moldoveanu, M. & Rau, I. Biopolymer thin films for photonics applications. *Electrochemistry and Physical Chemical Methods in Serving Materials for Sustainable Development* **415**, 33-36 (2009).

[97] Jiang, C. Y. *et al*. Mechanical properties of robust ultrathin silk fibroin films. *Advanced Functional Materials* **17**, 2229-2237 (2007).

[98] Sillen, C. W. M. P., Barendrecht, E., Janssen, L. J. J. & Vanstralen, S. J. D. Gas Bubble Behavior during Water Electrolysis. *Int J Hydrogen Energy* **7**, 577-587 (1982).

[99] Servoli, E., Maniglio, D., Motta, A. & Migliaresi, C. Folding and assembly of fibroin driven by an AC electric field: Effects on film properties. *Macromolecular Bioscience* **8**, 827-835 (2008).

[100] Frey-Wyssling, A. On the Density and the Optics of Silk Fibroin. *Biochim. Biophys. Acta* **17**, 155-156 (1955).

[101] Kluge, J. A., Rosiello, N. C., Leisk, G. G., Kaplan, D. L. & Dorfmann, A. L. The consolidation behavior of silk hydrogels. *Journal of the Mechanical Behavior of Biomedical Materials* **3**, 278-289 (2010).

[102] Wang, Y. Y., Cheng, Y. D., Liu, Y., Zhao, H. J. & Li, M. Z. The Effect of Ultrasonication on the Gelation Velocity and Structure of Silk Fibroin. *Silk: Inheritance and Innovation - Modern Silk Road* **175-176**, 143-148 (2011).

[103] Wang, X. Q., Kluge, J. A., Leisk, G. G. & Kaplan, D. L. Sonication-induced gelation of silk fibroin for cell encapsulation. *Biomaterials* **29**, 1054-1064 (2008).

[104] Zhao, H. P., Feng, X. Q., Yu, S. W., Cui, W. Z. & Zou, F. Z. Mechanical properties of silkworm cocoons. *Polymer* **46**, 9192-9201 (2005).

[105] Miura, M., Morikawa, H., Kato, H. & Iwasa, M. Analysis of the construction process of cocoon shape by Bombyx mori. *Journal of Sericultural Science of Japan* **66**, 23-30 (1997).

[106] Van der Kloot, W. G. & Williams, C. M. Cocoon Construction by the Cecropia Silkworm .1. the Role of the External Environment. *Behaviour* **5**, 141-156 (1953).

[107] Blossman-Myer, B. & Burggren, W. W. The silk cocoon of the silkworm, Bombyx mori: Macro structure and its influence on transmural diffusion of oxygen and water vapor. *Comparative Biochemistry and Physiology A-Molecular & Integrative Physiology* **155**, 259-263 (2010).

[108] Bissett, J. L. & Moran, V. C. The Life History and Cocoon Spinning Behavior of a South African Mantispid Neuroptera Mantispidae. *Journal of the Entomological Society of Southern Africa* **30**, 82-95 (1967).

[109] Lounibos, L. P. Initiation and Maintenance of Cocoon Spinning Behavior by Saturniid Silkworms. *Physiol. Entomol.* **1**, 195-206 (1976).

[110] Lounibos, L. P. Cocoon Spinning Behavior of Chinese Oak Silkworm, Antheraea-Pernyi. *Anim. Behav.* **23**, 843-853 (1975).

[111] Dominick, O. S. & Truman, J. W. The Physiology of Wandering Behavior in Manduca-Sexta .1. Temporal Organization and the Influence of the Internal and External Environments. *J. Exp. Biol.* **110**, 35-51 (1984).

[112] Ingram, A. L. & Parker, A. R. Structure, mechanism and mechanical properties of pupal attachment in Greta oto (Lepidoptera : Nymphalidae : Ithomiinae). *Entomol. Sci.* **9**, 109-120 (2006).

[113] Gowda, B. N. & Reddy, N. M. Effect of different environmental conditions on popular multivoltine x bivoltine hybrids of silkworm, Bombyx mori L. with reference to cocoon parameters and their effect on reeling performance. *Indian Journal of Sericulture* **45**, 134-141 (2006).

[114] Nishioka, T., Mase, K. & Kajiura, Z. The dispersion of the cocoon shape and its Mahalanobis's generalized-distance between races. *Journal of Insect Biotechnology and Sericology* **79**, 9-13 (2010).

[115] Miura, M., Morikawa, H., Shimizu, T., Mochizuki, S. & Iwasa, M. A stochastic model for the fixing and moving patterns of Bombyx mori in the cocoon construction process. *Journal of Sericultural Science of Japan* **68**, 55-63 (1999).

[116] Nishioka, T., Nakazawa, K. & Wai, C. K. Fundamental shape of the cocoon described with the Fourie cosine series determined by Akaike Information Criterion. *Journal of Sericultural Science of Japan* **70**, 11-15 (2001).

[117] Miura, M., Morikawa, H. & Sugiura, A. Statistical analysis of body movement and shape of Bombyx mori in spinning behaviour. *Journal of Sericultural Science of Japan* **64**, 237-245 (1995).

[118] Nishioka, T., Satoh, H. & Kurasawa, Y. Numeral description of the cocoon shape by principal component analysis using the fourier coefficients. *Journal of Sericultural Science of Japan* **67**, 479-484 (1998).

[119] Barton, S., Dandin, S. B. & Babu, G. K. S. Manufacture of Silk. PCT Patent Application WO 2005/049899, filed 12 Nov. 2004, and published 2 Jun. 2005.

[120] *http://www.cia.gov/library/publications/the-world-factbook/geos/xx.html*

[121] Hori, S. & Shimizu, I. Geoorientation and Photoorientation Behavior of Bombyx-Mori at Termination of Cocoon Construction. *Appl. Entomol. Zool.* **25**, 177-186 (1990).

[122] Kafatos, F. C. & Williams, C. M. Enzymatic Mechanism for Escape of Certain Moths from their Cocoons. *Science* **146**, 538-& (1964).

[123] Sanapapamma, K. J. & Naik, S. D. Contemporary breakthrough in Ahimsa silk spinning. *Indian Journal of Traditional Knowledge* **7**, 178-181 (2008).

[124] Edwards, W. F. Feeding Dyestuffs to Silkworms. *Textile World* **60**, 55-57 (1921).

[125] Campbell, F. L. Preliminary experiments on the toxicity of certain coal-tar dyes for the silkworm. *J. Econ. Entomol.* **25**, 905-917 (1932).

[126] Tansil, N. C. *et al*. Intrinsically Colored and Luminescent Silk. *Adv Mater* **23**, 1463-1466 (2011).

[127] Tansil, N. C., Han, M.-Y., Liu, X. Y., Soh R. & Li, Y. Intrinsically colored, luminescent silk fibroin and a method of producing the same. PCT Patent Application WO 2010/096025, filed 17 Feb. 2010, and published 26 Aug. 2010.

[128] Wenk, E., Merkle, H. P. & Meinel, L. Silk fibroin as a vehicle for drug delivery applications. *Journal of Controlled Release* **150**, 128–141 (2011).

[129] Simchua, W., Narkkong, N. A. & Baimark Y. Silk Fibroin Nanospheres for Controlled Gentamicin Sulfate Delivery. *Research Journal of Nanoscience and Nanotechnology* **1**, 34-41 (2011).

[130] *http://drugbank.ca/drugs/DB01045*

[131] *http://drugbank.ca/drugs/DB00798*

[132] Petrulyte, S. Advanced textile materials and biopolymers in wound management. *Danish Medical Bulletin* ***55***, 72-77 (2008).

[133] Gobin, A. S. Silk Fibroin Coating. US Patent Application US2009/162439, filed 22 Dec. 2008, and published 25 Jun. 2009.

[134] Lee, J. S., Lu, Y., Baer, G. S., Markel, M. D. & Murphy, W. L. Controllable protein delivery from coated surgical sutures. *Journal of Materials Chemistry* **20**, 8894-8903 (2010).

[135] Choi,H.-M., Bide, M., Phaneuf, M., Quist, W. & Logerfo, F. Antibiotic Treatment of Silk to Produce Novel Infection-Resistant Biomaterials. *Textile Research Journal* **74**, 333-342 (2004).

[136] Hines, D. J. & Kaplan, D. L. Mechanisms of Controlled Release from Silk Fibroin Films. *Biomacromolecules* **12**, 804-812 (2011).

[137] Kumar, J. S. & Kumar, N. S. Production Efficiency of Cocoon Shell of Silkworm, *Bombyx mori* L. (Bombycidae: Lepidoptera), as an Index for Evaluating the Nutritive Value of Mulberry, *Morus* sp. (Moraceae), Varieties. *Psyc*he **2011**, Article ID 807363, 3 pages (2011).

[138] Long, J. J., Wang, H. W., Lu, T. Q., Tang, R. C. & Zhu, Y. W. Application of Low-Pressure Plasma Pretreatment in Silk Fabric Degumming Process. *Plasma Chem. Plasma Process.* **28**, 701-713 (2008).

[139] Rajkhowa, R. *et al*. Structure and properties of biomedical films prepared from aqueous and acidic silk fibroin solutions. *Journal of Biomedical Materials Research Part A* **97A**, 37-45 (2011).

[140] Weisman, S. *et al*. Honeybee silk: Recombinant protein production, assembly and fiber spinning. *Biomaterials* **31**, 2695-2700 (2010).

[141] Jones, J., Rothfuss, H., Steinkraus, H. & Lewis, R. Transgenic goats producing spider silk protein in their milk; behavior, protein purification and obstacles. *Transgenic Res.* **19**, 135-135 (2010).

[142] Altman, G. H., Chen, J., Horan, R. & Horan, D. J. Sericin extracted fabrics. US Patent Application US 2010/0256756, filed 29 Apr. 2010, and published 7 Oct. 2010.

[143] Shelton, E. M. & Johnson, T. B. Researches on proteins. VII. The preparation of the protein "sericin" from silk. *J. Am. Chem. Soc.* **47**, 412-418 (1925).

[144] Long, J. J., Wang, H. W., Lu, T. Q., Tang, R. C. & Zhu, Y. W. Application of Low-Pressure Plasma Pretreatment in Silk Fabric Degumming Process. *Plasma Chem. Plasma Process.* **28**, 701-713 (2008).

[145] Ren Y., Chen Y.-Y., Ling H. & Yang J.-G. Effects of Treatment with Low-Temperature Oxygen Plasma on Silk Fiber Properties. *Silk Monthly* **47**(12), 10-19 (2002).

[146] Chen, Y., Lin, H., Ren, Y., Wang, H. & Zhu, L. Study on Bombyx mori silk treated by oxygen plasma. *J Zhejiang Univ Sci* **5**, 918-22 (2004).

[147] Lin, H. *et al*. Morphologies of Silk Fiber Treated by Plasma Under Different Condition. *Journal of Textile Research* **25**(4), 28-29 (2004).

[148] Park, D. J. *et al*. Sterilization of microorganisms in silk fabrics by microwave-induced argon plasma treatment at atmospheric pressure. *Surf. Coat. Technol.* **202**, 5773-5778 (2008).

[149] Hong, Y. J. *et al*. Non-thermal atmospheric pressure plasma sources for biomedical applications. *Proceedings of 2009 International Sympsium on Plasma Chemistry (ISPC 2010)*, P3.13.05 (2009).

[150] Bol'shakov, A. A. *et al*. Radio-frequency oxygen plasma as a sterilization source. *AIAA J.* **42**, 823-832 (2004).

[151] Adler, S., Scherrer, M. & Daschner, F. D. Costs of low-temperature plasma sterilization compared with other sterilization methods. *J. Hosp. Infect.* **40**, 125-134 (1998).